RSC Medicinal Chemistry

Accepted Manuscript

This article can be cited before page numbers have been issued, to do this please use: P. Jin, Md. M. Hasan, A. G.S. Pepper, S. Mitchell, K. M. Rahman and C. Pepper, *RSC Med. Chem.*, 2025, DOI: 10.1039/D5MD00316D.

ROYAL SOCIETY OF CHEMISTRY

rsc.li/medchem

View Article Online
DOI: 10.1039/D5MD00316D

Design, synthesis and evaluation of Pyrrolobenzodiazepine (PBD)-based PROTAC conjugates for the selective degradation of the NF-κB RelA/p65 subunit

Peiqin Jin[a], Md. Mahbub Hasan[a], Andrea G.S. Pepper[b], Simon Mitchell[b], Khondaker Miraz Rahman[a†], and Chris Pepper[a†].

[a]School of Cancer and Pharmaceutical Sciences, King's College London, London SE1 9NH, U.K.

[b]Brighton and Sussex Medical School, University of Brighton and University of Sussex, Brighton BN1 9PX, U.K.

[†]joint senior authors

KEYWORDS: proteolysis-targeting chimera (PROTAC), NF-κB, RelA/p65, pyrrolobenzodiazepine, anticancer drugs, triple negative breast cancer, leukaemia.

ABSTRACT: NF-κB signalling is frequently dysregulated in human cancers making it an attractive therapeutic target. Despite concerted efforts to generate NF-κB inhibitors, direct pharmacological inhibition of the kinases mediating canonical NF-κB has failed due to on-target toxicities in normal tissues. So, alternative strategies, designed to target specific components of the NF-κB signalling machinery, have the potential to selectively inhibit tumour cells whilst reducing the toxicities associated with broad inhibition of NF-κB in non-malignant cells. Here we present evidence that a C8-linked pyrrolobenzodiazepine (PBD) containing proteolysis-targeting chimera (PROTAC) selectively degrades the NF-κB subunit, RelA/p65 in a proteasome-dependent manner. Our lead PROTAC (JP-163-16, **15d**) showed cytotoxicity with mean LC_{50} values of 2.9μM in MDA-MB-231 cells, 0.14μM in MEC-1 cells and 0.23μM in primary chronic lymphocytic leukaemia cells. In contrast, **15d** was two-logs less toxic in primary B- and T-lymphocytes (mean LD_{50} 19.1μM and 36.4μM, respectively). Importantly, the development of **15d**, by conjugating the C8-linked PBD with a cereblon-targeting ligand using a five-carbon linker, abolished the ability of the C8-linked PBD to bind to DNA, whilst demonstrating cytotoxicity in cancer cells associated with the degradation of RelA/p65. Mechanistically, **15d** displayed PROTAC credentials through the selective degradation of NF-κB RelA/p65 in a proteasome-dependent manner and showed a five-fold reduction in potency in the cereblon deficient, lenalidomide resistant, myeloma cell line, RPMI-8226. To our knowledge, this work describes the first PROTAC capable of selective degradation of a single NF-κB subunit and highlights the therapeutic potential of our strategy for the treatment of RelA/p65-dependent tumours.

INTRODUCTION

The nuclear factor kappa-light chain-enhancer of activated B-cell (NF-κB) is a transcription factor that plays a pivotal role in inflammatory and immune responses, and its abnormal activation is associated with various pathogenic effects[1,2]. For example, an over-expressed level of NF-κB signalling contributes to metastasis in triple-negative breast cancer (TNBC) [3]. In haematological malignancies, elevated nuclear expression of the NF-κB subunit RelA/p65 is commonly associated with more aggressive tumour cell growth increased tumour burden and the emergence of drug resistance[4]. Given the pivotal role that NF-κB plays in the development and progression of a range of human cancers, it seems logical to develop strategies to target abnormal NF-κB signalling for the treatment of these diseases[5].

However, direct targeting of transcription factors (TFs), has long been considered intractable due to the lack of well-defined enzymatic binding pockets and limited H-bond donors and acceptors, rendering them 'undruggable'[6,7]. To date, only a small number of molecules have been shown to be capable of interacting with NF-κB [8]. One such molecule, (-)-DHMEQ, a synthetic compound derived from epoxyquinomicin C, can inhibit the nuclear transport of the transcriptional subunit RelA/p65 (Figure 1a)[9]. Unfortunately, further development of this compound series was halted due to pharmacokinetic issues[10].

Pyrrolobenzodiazepines (PBDs) (Figure 1b) are highly cytotoxic agents derived from Streptomyces [11]. They exert their primary anti-tumour effect by selectively binding into the minor groove of DNA in a sequence-selective manner. Subsequent studies showed that these compounds were also able to target DNA motifs related to TF signalling[11,12]. Hu et al synthesized a C8-conjugated PBD hybrid named IN6CPBD, and cellular studies revealed that this compound induced cellular apoptosis in A375 cells by repressing activation of NF-κB[13]. Similarly, KMR-28-39 (also named 'TSG-1301') was shown to interfere with the binding of NF-κB protein to its cognate DNA motifs [11,14] (Figure 1c). This competitive inhibition resulted in nanomolar cytotoxicity in leukaemia cells[14]. Further SAR studies showed that compound 13 (Figure 1d) caused a high level of inhibition of RelA/p65-DNA binding in chronic lymphocytic leukaemia (CLL) cells[12,14]. Other molecules like CRL1101 and IT-901 (Figure 1e-f), were also reported to block NF-κB subunits RelA/p65 and c-Rel[8,15] but none of these compounds have been approved for use as anticancer agents.

Recently, proteolysis targeting chimeras (PROTACs) have emerged as a promising alternative strategy for selectively interfering with the activity of TFs like NF-κB. Unlike traditional small molecule inhibitors or antibodies, PROTACs recruit the ubiquitin-protease system to break down a specific protein of interest (POI), leading to target protein degradation (TPD). The PROTAC recognises the

View Article Online
DOI: 10.1039/D5MD00316D

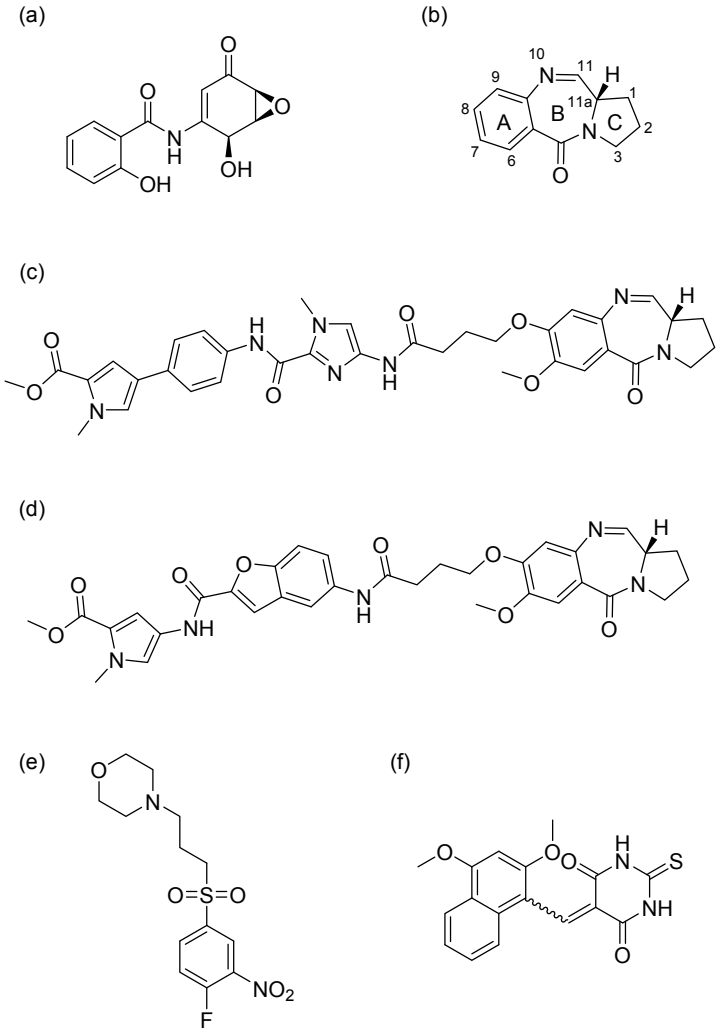

Figure 1. Chemical structure of reported NF-κB targeting compounds (-)-DHMEQ, PBD core, KMR-28-39 (TSG-1301), Cpd 13, CRL1101, and IT-901.

protein target via its POI ligand, while the E3 ligand located at the other end of the molecule will bring an E3 ligase proximate to the target substrate for consequent POI ubiquitination[16,17]. This ubiquitinated protein is subsequently degraded in the proteasome[16,17]. Due to their distinct mechanism of action,

PROTACs can target non-druggable proteins that lack enzymatic activities, such as TFs, and they do not need to be maintained at high concentrations to induce their therapeutic effect[18–20], which can diminish on-target toxicity concerns[18–20]. PROTACs also have the potential to re-sensitise cancer cells to chemotherapy due to their ability to degrade proteins associated with drug resistance[21]. Considering these unique therapeutic characteristics, PROTAC technology has the potential to expand the library of drug candidates for clinical purposes. Indeed, PROTACs have already shown remarkable ability to promote anti-cancer activity[18].

This project set out to develop PROTACs that can selectively degrade the NF-κB protein RelA/p65. The objective was to deplete this single NF-κB subunit, which is over-expressed in some cancer cells[4,5], whilst preserving the other components of the NF-κB signalling machinery. In so doing, we hoped to selectively target the tumour cells and diminish on-target toxicities in normal cells. Although other researchers have developed NF-κB targeting PROTACs[22], to-date there are no reports of PROTACs that are able to selectively degrade a single NF-κB subunit. Although PBDs are well-characterised DNA interacting agents, more recently, C8-conjugated PBDs have been shown to also interact with proteins.[23] We used PBD derivatives that were shown by *in silico* modelling to be able to bind to RelA/p65 (Figure 2). The PBDs were then conjugated with cereblon (CRBN)-recruiting PROTAC building blocks via multi-step

View Article Online
DOI: 10.1039/D5MD00316D

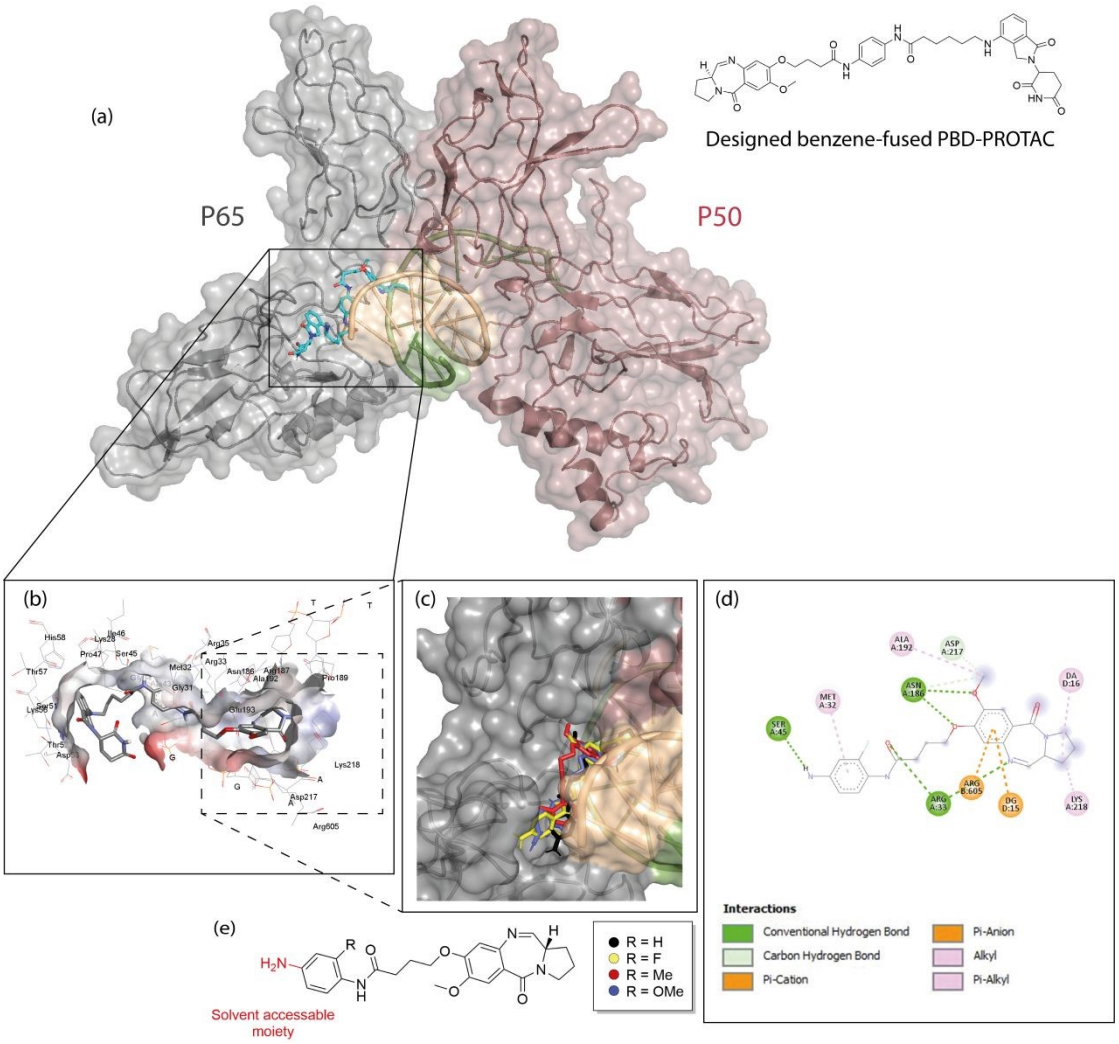

Figure 2. Docking of PBD-PROTAC with the RelA/p65-p50-DNA complex (PDB:1VKX) (a) Molecular docking of designed PBD-PROTAC (**15d**) zoomed in figure showing the **15d** binding pose in the RelA/p65-DNA binding interface (c) Overlapped docking results of PBD controls within RelA/p65-DNA interface (d) The typical 2D ligand-interface binding projection of PBD ligands. Here fluorine-substituted PBD (JP-19-12) was selected as an example, while the dashed lines highlight the protein-ligand interactions. (e) Chemical structure of the docked PBD building blocks.

synthetic routes. These synthesised molecules were then biologically screened for their toxicity in cancer cells and non-malignant B- and T-lymphocytes. Subsequently, preliminary investigations were carried out to establish their mechanism of action.

RESULTS AND DISCUSSIONS

Design and Synthesis of RelA/p65-targeting PROTACs To design NF-κB targeting PROTACs, C8-conjugated PBD molecules were selected as RelA/p65-targeting ligands as these C8-phenyl linked short PBDs had been previously shown to inhibit the activity of the canonical RelA/p65 NF-κB subunit, implying their potential as NF-κB-targeting POI ligands[12]. The initial concept was to produce RelA/p65-targeting PROTACs that were linked to CRBN-based building blocks. For a PROTAC to work, it's two functional components must be connected by a linker. One part of the molecule selectively binds the target protein, whilst the second part of the molecule recruits a cellular enzyme, an E3 ligase. This enables the PROTAC to recruit an E3 ligase enzyme into close contact with the target protein, enabling the protein to be marked for degradation in the cellular proteasome. Previous research on early-stage PROTAC

View Article Online
DOI: 10.1039/D5MD00316D

Scheme 1. Synthesis of (a) lenalidomide-based CRBN building block JP-163-05 (b) PBD core (c) PBD-based PROTACs[12,14]

(a)

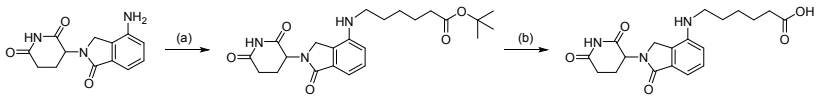

1
JP-163-03

2
JP-163-05

(a) tert-Butyl 6-bromohexanoate, DIPEA, NMP, 130°C, o/n (Yield: 78.3%) (b) TFA, DCM, 1h

(b)

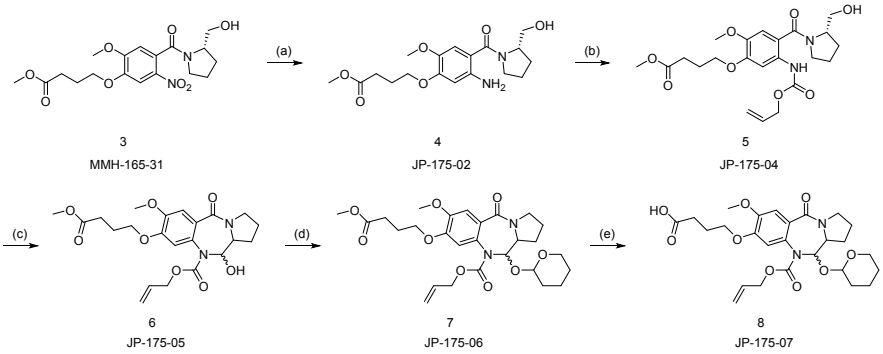

3
MMH-165-31

4
JP-175-02

5
JP-175-04

6
JP-175-05

7
JP-175-06

8
JP-175-07

(a) Pd-C, NH_4HCO_2, EA/EtOH = 1/1, H_2 at 40 Psi, 4h (b) Allylchloroformate, pyridine, DCM (anhydrous), 2h (Yield: 47.6%)
(c) TEMPO, BAIB, DCM, 6h (Yield: 67.2%) (d) DHP, PTSA, EA, 2h (Yield: 90.1%) (e) 2M NaOH, Dioxane, 2h

(c)

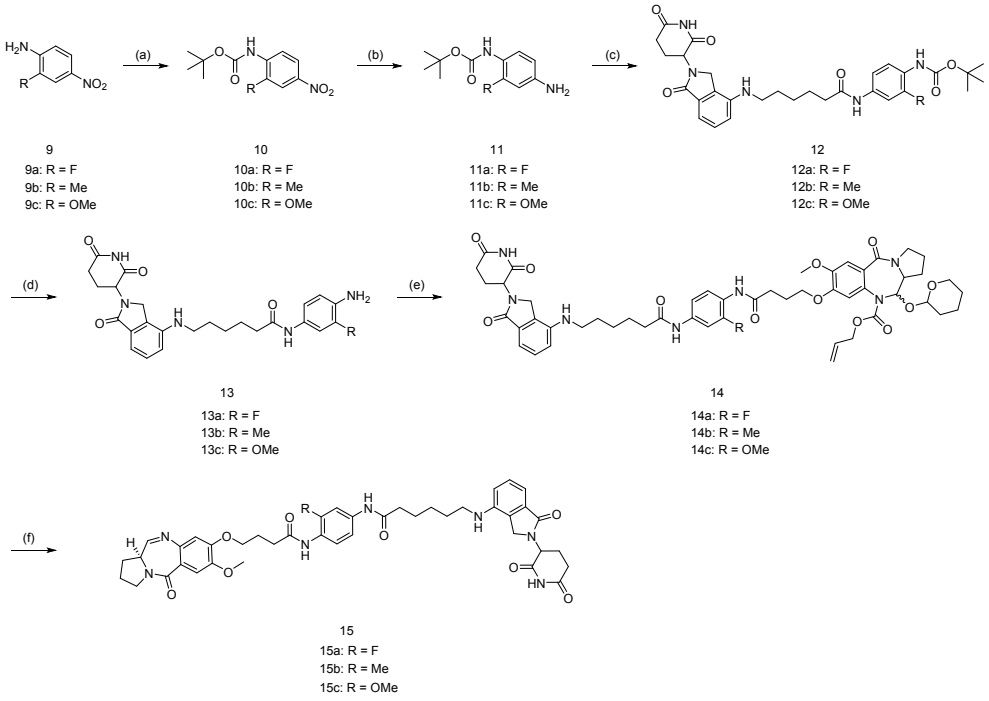

9
9a: R = F
9b: R = Me
9c: R = OMe

10
10a: R = F
10b: R = Me
10c: R = OMe

11
11a: R = F
11b: R = Me
11c: R = OMe

12
12a: R = F
12b: R = Me
12c: R = OMe

13
13a: R = F
13b: R = Me
13c: R = OMe

14
14a: R = F
14b: R = Me
14c: R = OMe

15
15a: R = F
15b: R = Me
15c: R = OMe

(a) Di-tert-butyl decarbonate, TEA, DMAP, DCM, r.t, o/n (Yield: 35.0-59.7%) (b) Pd-C, NH_4HCO_2, EtoAc/EtOH = 2/3, H_2 at 40 Psi, o/n
(c) JP-163-05, DMAP, EDC, DMF, o/n (Yield: 18.5-36.6%) (d) TFA, DCM, 1h
(e) JP-175-07, DMAP, EDC, DMF (anhydrous), o/n (Yield: 44.1-44.3%)
(f) Pyrrolidine, PPh_3, DCM, palladium tetrakis[triphenylphosphine], r.t., 2h (Yield: 67.1-99.0%)

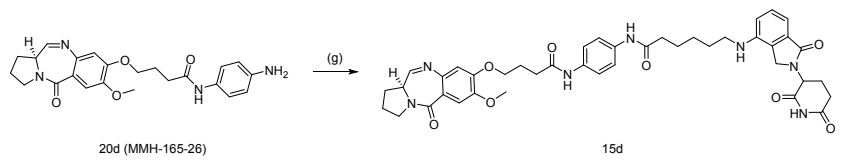

20d (MMH-165-26)

15d

(g) 2, DMAP, EDC, DMF, o/n (Yield: 7.4%)

View Article Online
DOI: 10.1039/D5MD00316D

Scheme 2. Synthesis of PBD controls.

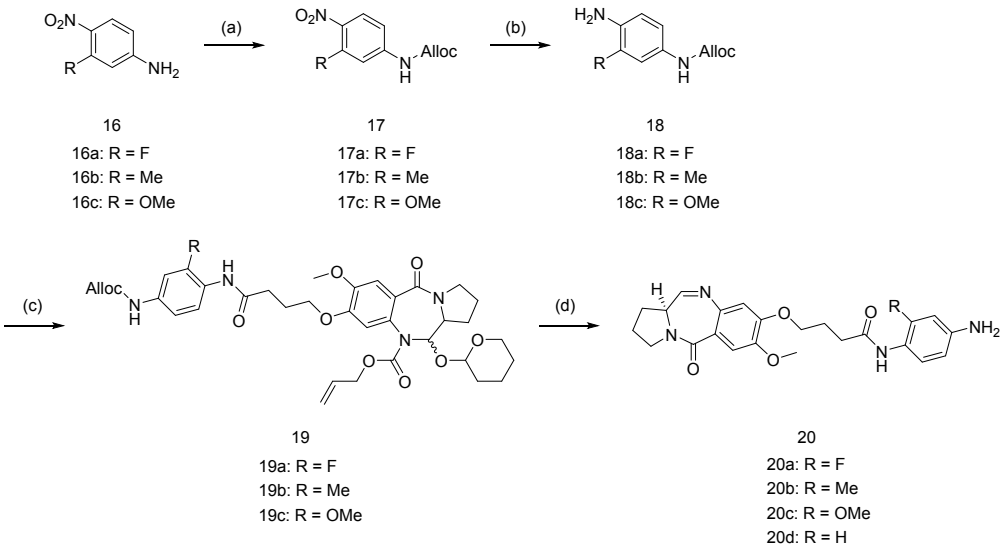

(a) K_2CO_3, THF, Allyl chloroformate, r.t., o/n (Yield: 72.7-83.7%)
(b) Fe, NH_4Cl, $EtOH/H_2O$ = 3/1, 80°C, 2h
(c) JP-175-07, DMAP, EDC, DMF, o/n (Yield: 96.0-98.4%)
(d) Pyrrolidine, PPh_3, DCM, palladium tetrakis[triphenylphosphine], r.t., 2h (Yield: 29.9-98.5%)

design used a linear chain of alkyl units as a linker, which allowed the length of the linker to be modified (typically 5-11 carbon chain)[17,22,24,25]. Here, we selected a 5-carbon aliphatic linker for our preliminary study as molecular modelling suggested that this would allow the CRBN-ligand (lenalidomide) to be bioavailable once the POI had been captured. The designed structure and the docking simulation are shown in Figure 2 (PBD: 1VKX). It was noted that the PBD moiety was stabilized at the interface between DNA segment and RelA/p65 NF-κB subunit, while the CRBN ligand domain protruded outside the structure, suggesting that it would remain accessible for CRBN binding. Given the substantial interactions with RelA/p65, we hypothesized that this PBD molecule may have sufficient RelA/p65 binding to serve as a POI ligand.

The expanded figure shows that the POI ligand binds in the RelA/p65 domain between Glu193 to Lys218 (Figure 2b). Further investigation of the short C8-phenyl linked short PBD molecules suggested a similar binding pattern where the PBD core resides inside, and the aniline moiety is relatively solvent-exposed (Figure 2c, d). To synthesize the molecules, the synthetic scheme of the PROTAC building block was based on the conditions reported by Qiu et al (Scheme 1a)[26]. The PBD core was then synthesized as RelA/p65-targeting ligands as shown in Scheme 1b[12,14]. PBD-based PROTACs were generated as shown at Scheme 1c. Di-tert-butyl decarbonate was used to install a Boc-protecting group towards the exposed amine of starting material **9**. The product **10** underwent nitro reduction catalysed by Pd-C, while the reduced amine was then attached to the PROTAC building block **2** to generate **12**. In the next step, TFA was used to deprotect the Boc group and the product was thus coupled with PBD core via EDC/DMAP mediated amide coupling reaction. Finally, the THP and alloc protecting groups were simultaneously removed via pyrrolidine and tetrakis(triphenylphosphine)palladium(0), to obtain the final series **15a-15c**. **15d** was directly synthesized via EDC/DMAP mediated amide coupling reaction. For the synthesis of PBD control **20a-20d**, the aromatic-substituted amine was initially conjugated to the PBD core via an amide coupling reaction, and the products were obtained by removing THP and alloc protecting groups (Scheme 2). The cytotoxicity of the synthesised PROTACs were compared with the individual constituent PBD controls.

15d exhibits cytotoxicity in MEC-1 cells. To evaluate the therapeutic potential of the PBD-PROTACs and their constituent PBD building blocks, all samples were tested in the chronic lymphocytic leukaemia (CLL) cell line, MEC-1. Cells were exposed to PROTACs or their PBD building blocks for 48h, and drug-induced apoptosis was quantified using Annexin V and 7-AAD labelling using flow cytometry. Given the known DNA-binding characteristics of PBDs, we used a FRET-melting assay to compare the ability of the PROTAC molecules and their constituent PBD molecules to interact with DNA. All compounds were serially diluted (10μM) and then added to annealed FAM-TAMRA labelled AT-rich single stranded hairpin

View Article Online
DOI: 10.1039/D5MD00316D

Table 1. Cytotoxic activities in MEC-1 cell line and DNA-binding characteristics of the PBD-based PROTACs and their PBD building blocks.

PROTAC	MW	LC_{50} (μM)	ΔTm (°C)	PBD building blocks	MW	LC_{50} (μM)	ΔTm (°C)
15d (JP-163-16)	777.88	0.14 ± 0.02	-0.82	**20d** (MMH-165-26)	422.49	0.31 ± 0.14	1.25
15a	795.87	0.81 ± 1.47	1.05	**20a**	440.48	0.03 ± 0.29	2.17
15b	791.91	0.84 ± 0.48	0.73	**20b**	436.51	1.18	-0.06
15c	807.91	>1000	1.27	**20c**	452.51	1.31 ± 0.74	0.70

DNA. DNA Engine Opticom was used to determine the DNA melting characteristics. The sample was initially incubated at 30°C for 3h and then gradually increased to 100°C. The FAM-TAMRA fluorescent signal was detected at 0.5°C intervals and the mean melting point was determined using GraphPad Prism software. The melting point difference between each compound and naked ssDNA (ΔTm) was calculated for comparison.

The screening results are presented in Table 1, and the dose-response curves were attached in Figure. S12. Compound **15d** showed the highest anti-tumour effects in MEC-1 cells. The result of the FRET-melting assay is shown in Figure 3. 50 equivalents of PBD (10μM) induced the shift of melting point of the DNA by ΔTm of 1.25°C, whereas the same equivalence of PROTAC compound **15d** showed almost no change in ΔTm, suggesting that these compounds do not interact with DNA. Consequently, the high toxicity of **15d** in cancer cell lines and primary CLL cells, is unlikely to be attributable to the ability of the PROTAC to bind to DNA. These data suggest a distinct mechanism of action of the PROTAC when compared to its PBD building block.

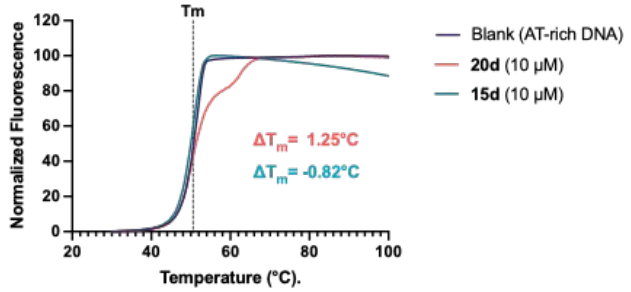

Figure 3. FRET melting assay results reveal that the PROTAC (15d) does not significantly interact with DNA. Each compound was mixed with an AT-rich DNA sequence at 10μM. 15d did not increase the melting temperature suggesting that it does not interact with DNA. In contrast, the PBD building block (20d) caused a marked increase in DNA melting temperature, confirming its ability to bind to and stabilise DNA.

15d causes RelA/p65 degradation in a proteasome-dependent manner. To further explore the relative potency and mechanism of action of **15d**, the lead PROTAC molecule was tested in MEC-1 cells, primary CLL cells derived from patients (n=8) and normal B- and T-lymphocytes (n=5). Cells were exposed to **15d**, its PBD building block **20d**, or lenalidomide for 48h and drug-induced apoptosis was quantified using the same assay as described above. **15d** and **20d** showed potent anti-tumour effects in MEC-1 cells, while lenalidomide had a negligible impact on MEC-1 cell viability (Figure 4a). Primary CLL cells were also sensitive to the apoptotic effects of **15d**. In contrast, normal B- and T-lymphocytes were more than two logs less sensitive to the effects of the PROTAC (Figure 4b). In parallel experiments, RelA/p65 expression was measured in MEC-1 cells treated with **15d** or **20d**. Figure 4c-4e show that both agents induced a marked reduction in RelA/p65 expression. However, the dose-response patterns of the two molecules were different. **20d** induced a dose-dependent reduction in RelA/p65 expression. In contrast, **15d** showed a similar reduction in RelA/p65 with all the concentrations tested. This supports the concept that **15d** may have catalytic properties, which enable the recycling of PROTAC molecules after the target protein is degraded. In contrast, the PBD, **20d**, demonstrated an occupancy-driven mechanism of action; a more obvious concentration-dependent reduction in RelA/p65 was observed in MEC-1 cells treated with **20d**. Given its known DNA-binding activity, it seems likely that dose-dependent minor groove binding contributes to the cytotoxicity of **20d**, which could, in turn, result in higher levels of competitive blockade of RelA/p65 DNA binding sites[12,27]. In contrast, the PROTAC molecule, **15d**, appeared to induce an event-driven pharmacology consistent with POI degradation. Interestingly, although the PROTAC induced similar levels of RelA/p65 reduction at both 0.25μM and 1μM, the higher concentration of **15d** induced a stronger anti-tumour effect. This unique pattern could be caused by the 'hook effect' frequently observed with PROTAC compounds [20,27,28].

To confirm the proteasome dependency on the cytotoxic effects of **15d** in MEC-1 cells, cells were co-treated with the proteasome inhibitor MG-132. We initially established the cytotoxic and proteasome inhibitory effects of MG-132 in MEC-1 cells (Figure 4f). MEC-1 cells were treated with increasing concentrations of the proteasome inhibitor, MG-132 (0.1μM – 2.5μM) for 48h. Aliquots of cells were first assessed for their apoptotic response to MG-132

View Article Online
DOI: 10.1039/D5MD00316D

using annexin V and 7-AAD labelling. In parallel, proteasome activity was evaluated using a proteasome activity assay kit (Abcam). The kit uses an AMC-tagged peptide substrate (Proteasome Substrate (Succ-LLVY-AMC in DMSO), which releases free, highly fluorescent AMC (Ex/Em 350/440 nm) in the presence of proteolytic activity. Due to the high sensitivity of MEC-1 cells to the effects of MG-132, a concentration of 0.18 µM MG-132 was used in combination with **15d** or **20d**.

This concentration of MG-132 reduced cellular proteasome activity by approximately 40-50% without inducing significant apoptosis. Each experiment was repeated five times in duplicate, and the mean LC_{50} values were calculated for each experiment. Subsequently the matched LC_{50} values (+/- the addition of MG-132) were plotted and the difference between the LC_{50} values was determined using the paired t-test (Figure 4g and 4h). The results indicate that blocking the proteasome significantly repressed the cytotoxicity of **15d** ($p<0.05$), while there was no significant difference in LC_{50} values when MG-132 was co-administered with the PBD **20d**. This provided further evidence that the anti-tumour effect of **15d** is caused, at least in part, by proteasome-dependent degradation of RelA/p65. However, it should be noted that **15d** was not able to entirely deplete the cellular expression of this molecule. Although molecular modelling showed excellent binding characteristics of the PBD PROTAC with RelA/p65, it may not result in the optimal degradation of RelA/p65 [12]. The scale of target protein degradation is reliant on the stability and positive cooperativity of the ternary complex, so a ligand bearing an inferior binding affinity could still induce effective protein degradation with considerable selectivity[19,20]. Issues like charged repulsion between the E3 ligase and POI or steric clashes induced by unfavourable PROTAC conformation are more likely to be the cause of the incomplete RelA/p65 degradation[7,18,19]. Although we did not directly explore ternary complex formation i.e., the binding of the PROTAC to both the protein of interest (RelA/p65) and the target E3 ligase (CRBN), we did examine the cytotoxic effects of **15d** in the multiple myeloma cell line, RPMI-8226. These cells have very low CRBN protein expression and are consequently resistant to lenalidomide.[29] Using these cells we were able to confirm that the mechanism of action of **15d** is, at least in part, dependent on CRBN; the PROTAC showed a five-fold reduction in efficacy in RPMI-8226 cells (Figure 4i). In contrast, the PBD building block **20d** showed similar cytotoxicity in RPMI-8226 cells and MEC-1 cells (Figure 4j) confirming that its cytotoxic effects were independent of CRBN.

Previous research indicated that PBD molecules fused with benzofuran and pyrrole terminal were selective for RelA/p65 inhibition. In contrast, benzene-fused short PBDs caused very limited RelA/p65 perturbance, but with significant effects on other NF-κB subunits[12]. Consequently, the effect of **15d** was evaluated on other NF-κB subunits (RelB and cRel) as described below.

15d selectively degrades the NF-κB RelA/p65 subunit. To ascertain the selectivity of **15d** for the degradation of the RelA/p65 NF-κB subunit, MEC-1 cells were treated for 24 hours a range of concentrations of **15d** (0-1µM). Cells were then harvested, fixed and permeabilised and labelled with fluorescence-labelled antibodies against, the NF-κB subunits p65 (APC), RelB (Corallite 488) and cRel (PE). Protein expression was quantified using a CytoFLEX LX flow cytometer. Figure 5 shows that **15d** induced a marked reduction in RelA/p65 expression at 0.5µM and 1µM. In contrast, no significant change in RelB was observed at the same concentrations. Although a small but significant reduction in cRel was noted at 0.5µM, this was not replicated at 1µM. This suggests that **15d** selectivity depletes RelA/p65, which adds to its promising characteristics as a lead PROTAC compound. To our knowledge, **15d** represents the first example of a RelA/p65 selective PROTAC that does not substantially impact RelB or cRel.

Effects of PROTAC 15d on MDA-MB-231 cell viability. We next investigated the potency of **15d** in the triple-negative breast cancer cell line (MDA-MB-231). This cell line was selected as it over expresses RelA/p65 and represents a cancer type with significant clinical unmet need [30,31]. As shown in Figure 6a, **15d** was more potent than its constituent molecules, the POI targeting PBD, **20d** and the CRBN E3 ligase ligand, lenalidomide. The cells were treated with serial dilutions of each compound and then incubated for 48 hours. FITC Annexin V and 7-AAD labelling was used to evaluate cell viability using flow cytometry. In keeping with our findings in MEC-1 and primary CLL cells **15d** and MMH-165-26 both demonstrated high tumour suppressive effects in cancer cells with LC_{50} values in the low micromolar range, **15d** was significantly more potent than its PBD building block, **20d** (Figure 6c). The CRBN ligand, lenalidomide, showed low cytotoxicity even at the highest concentration tested.

15d promotes the degradation of RelA/p65 in MDA-MB-231 cells in a proteasome-dependent manner. Next, to confirm the PROTAC mechanism of action of **15d**, MDA-MB-231 cells were co-treated with the proteasome inhibitor, MG-132 to evaluate whether this altered the tumour suppressive effects[32]. MG-132 was much less cytotoxic in MDA-MB-231 cells when compared with MEC-1 cells, and again a concentration of MG-132 was selected that did not have significant cytotoxicity but inhibited proteasome activity by approximately 50% (Figure 7a)[33]. Analysis of the cytotoxic dose-response curves and the impact of MG-132 on proteasomal activity in MDA-MB-231 cells revealed that 1µM MG-132 caused >50% reduction in proteasome activity in MDA-MB-231 cells without inducing a significant reduction in cell viability when compared with the untreated controls (Figure 7a and 7b). Based on the evaluation of the effects of MG-132 in MDA-MB-231 cells, cells were then treated with **15d**, **20d** and lenalidomide, with and without the addition of 1µM MG-132.

View Article Online
DOI: 10.1039/D5MD00316D

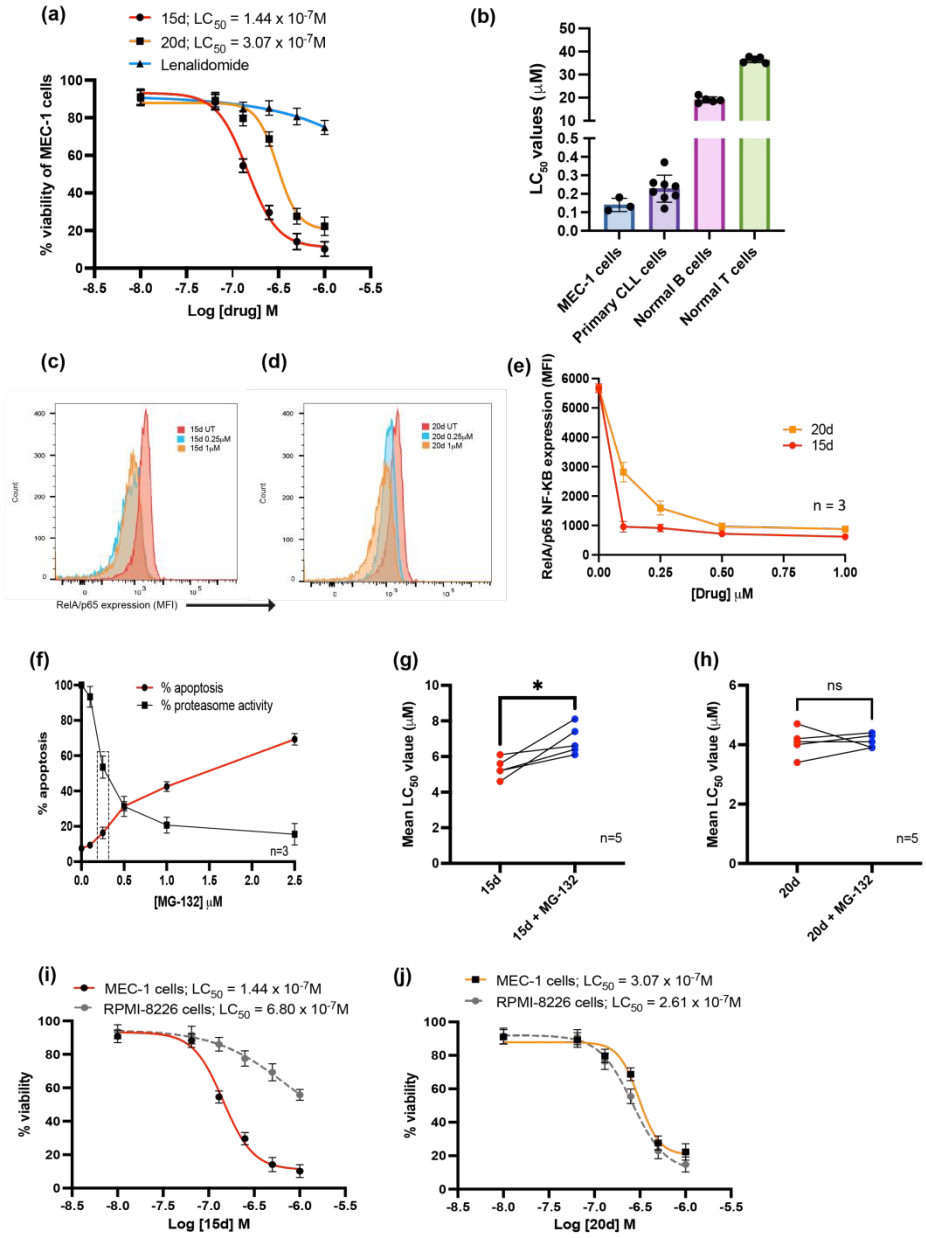

Figure 4. (a) Overlaid dose-response curves for **15d**, **20d**, and lenalidomide in the MEC-1 cell line. Dose-response curves were generated using annexin V/7-AAD data following 48h of exposure to each compound. The LD_{50} values were interpolated from each individual dose-response curve using GraphPad Prism 10, with all experiments performed in triplicate. (b) Shows the relative cytotoxic effect of **15d** in MEC-1 cells, primary CLL cells and normal B- and T-lymphocytes. Normal lymphocytes were more than two logs less sensitive to the effects of **15d** when compared with malignant B cells. RelA/p65 expression was significantly reduced in MEC-1 cells treated for 24h with (c) **15d** and (d) **20d**. (e) In contrast to **20d**, **15d** did not show a dose-dependent reduction in RelA/p65, which suggests an event-driven mechanism of action consistent with other PROTACs. Furthermore, co-treatment with the proteasome inhibitor, MG-132, demonstrated a proteasome-dependent mechanism of action of (f) The cytotoxic and proteasome inhibitory effects of MG-132 were evaluated in MEC-1 cells and a concentration of 0.18μM was chosen for the subsequent combination studies. (g) **15d** shows a proteasome dependent mechanism of action. (h) In contrast, the PBD building block, **20d**, showed a proteasome-independent mechanism of action. (i) The cytotoxic effects of 15d were shown to be dependent on CRBN expression by the five-fold reduction in potency in the CRBN deficient myeloma cell line, RPMI-8226. (j) in contrast, the PBD building block, 20d, showed similar potency in RPMI-8226 cells. All LC_{50} values were interpolated from individual dose-response curves using GraphPad Prism 10. Results are shown as the mean of five independent experiments carried out in duplicate. Statistical significance was determined using paired t-tests * $p<0.05$.

View Article Online
DOI: 10.1039/D5MD00316D

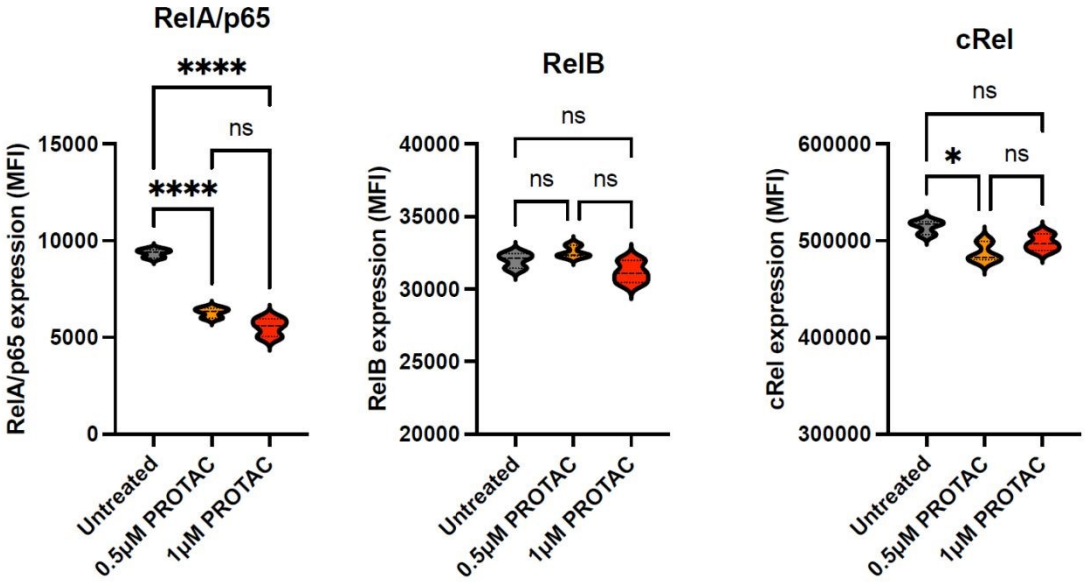

Figure 5. Comparison the effect of **15d** (PROTAC) on the expression of three NF-κB subunits RelA/p65, RelB and cRel. Each subunit was quantified using fluorescence-labelled antibodies All experiments were performed three times in duplicate and data are presented as violin plots. Statistical significance was determined using the Kruskal-Wallis test with Dunn's multiple comparison *post hoc* correction. * p<0.05, ** p<0.01, *** p<0.001, ****p<0.0001.

Co-treatment with MG-132 significantly reduced the cytotoxic effect of **15d**, which indicated a proteasome-dependent mechanism of action (Figure 7c). In contrast, MG-132 did not significantly alter the cytotoxicity of **20d**, implying again that the mechanism of action of this PBD compound was independent of proteasomal function (Figure 7d). In the case of lenalidomide, blocking proteasome activity increased its cytotoxicity, but this was not statistically significant (Figure 7e)[33]. This result indicated the mechanism of the PBD was distinct from that of **15d** as it was not dependent on proteasomal activity. As a C8-linked short PBD, **20d** can bind into the minor groove of DNA and form a covalent bond with guanine molecules. This may contribute to its effect on NF-κB as it facilitates sequence-selective binding at promoter regions containing the guanine-rich NF-κB binding motifs, thereby disrupting NF-κB signal transduction[11,12,34]. In this case, **20d** may retain its anti-tumour activity after the blockade of proteasome function.

As for the E3 ligase ligand, lenalidomide, used to develop **15d**, it did not significantly induce cell death as a single agent, but co-administration of MG-132 mildly improved tumour suppression. This could be caused by the additive impact of combination treatment as lenalidomide promote immune cell activation that might slightly improve tumour sensitivity to other agents bearing distinct mechanisms, like MG-132[35–37]. Subsequently, the ability of **15d** to reduce RelA/p65 expression in MDA-MB-231 cells was evaluated using flow cytometry. Cells were treated with increased concentration of **15d** for 24h, and then they were harvested and permeabilised followed by labelling with an APC-labelled RelA/p65 antibody. A significant reduction in RelA/p65 expression was observed after treating with 0.5μM and 1μM **15d**, which when co-administrated with 1μM MG-132 reversed this effect; consistent with a proteasome-dependent mechanism of action (Figure 4f). It was noted that 0.5 μM administration of **15d** caused a similar depletion of RelA/p65 as that achieved with 1 μM. Due to the bifunctional characteristic of PROTAC molecules, high intracellular levels of PROTAC may lead to saturated binding of its relative binary complexes, which competitively restricts the forming of the effective ternary complex required for target protein degradation[20,27,28,38]. It is possible that **15d** saturated the binding sites of RelA/p65 and/or CRBN in MDA-MB-231 cells at 1μM, which may restrict the formation of the POI-PROTAC-E3 complex thereby limiting the capacity for RelA/p65 degradation[20,28]. In summary, **15d** induced cytotoxicity in MDA-MB-231 cells and promoted the degradation of the RelA/p65 in a proteasome-dependent manner.

View Article Online
DOI: 10.1039/D5MD00316D

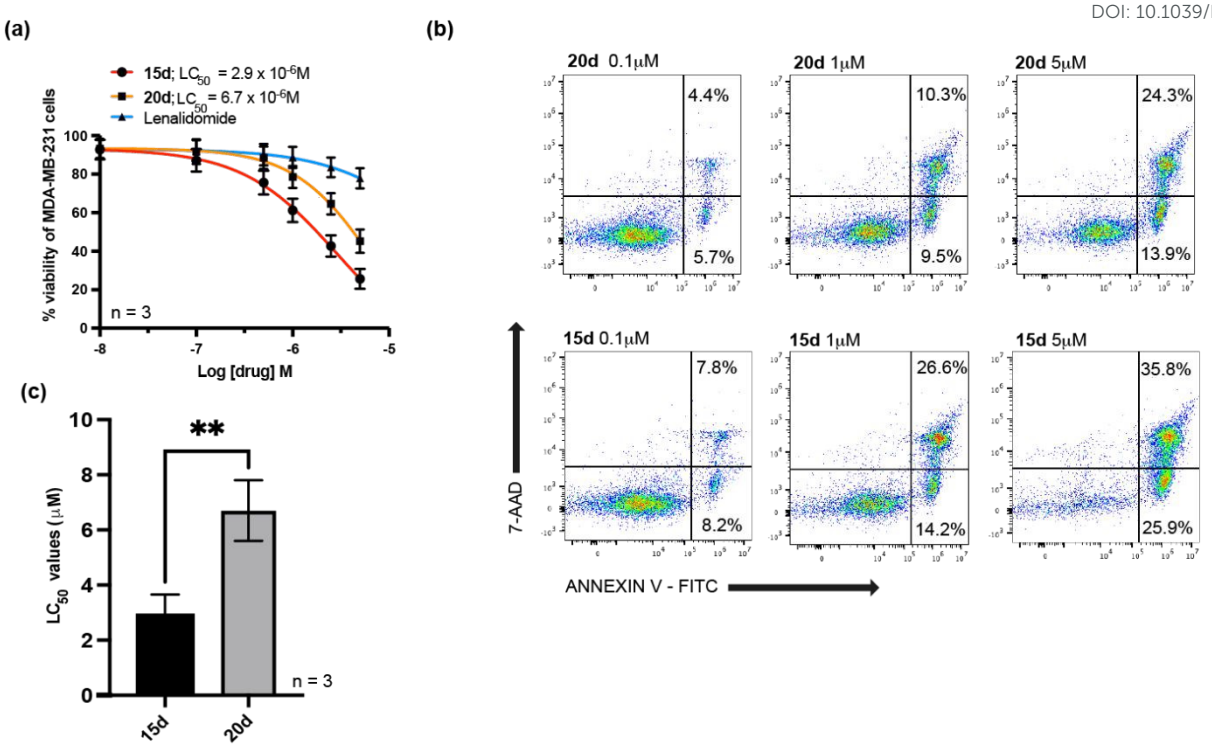

Figure 6. Evaluation of **15d** in MDA-MB-231 cells (a) Dose-response curves for **15d**, **20d**, and lenalidomide in MDA-MB-231 cells. Cells were treated with a range of concentrations of the PROTAC (**15d**) and the individual constituent molecules (**20d** and lenalidomide). Dose-response curves were generated using Annexin V/7-AAD data following 48h of exposure to each compound. The LC_{50} values were interpolated from each individual dose-response curve using GraphPad Prism 10. All experiments were performed in triplicate. (b) shows an example of the gating strategy used to identify viable and apoptotic MDA-MB-231 cells. The percentage of viable cells was defined by cells being Annexin-V and 7AAD negative. (c) The mean LC_{50} values (+SD) for **15d** and **20d** are shown for three independent experiments carried out in triplicate. **15d** was significantly more cytotoxic than **20d** **p<0.001.

CONCLUSIONS

Targeting the NF-κB signalling pathway has long been an appealing therapeutic strategy due to its role in regulating a range of cellular processes. The aberrant protein expression of one or more NF-κB subunits often results in increased NF-κB signalling, which is associated with pathogenic effects such as tumour proliferation, angiogenesis, and drug resistance. Here, we report the first prototype PROTAC capable of selectively degrading the NF-κB subunit RelA/p65. The POI targeting ligand was a C8-linked short PBD; simulated docking experiments showed strong binding to RelA/p65 protein in a region the protein predicted to interact with NF-κB DNA motifs. This supported its use as a selective ligand for targeting RelA/p65 protein if incorporated into a bifunctional PROTAC molecule. Consequently, PBD molecules were conjugated with a lenalidomide-based building block via an amide coupling reaction. A series of PBD PROTACs were synthesized, and all final products were purified either by flash column chromatography or preparative chromatography. Biological screening indicated that the lead compound, **15d**, showed potency in the TNBC breast cancer cell line, MDA-MB-231 (LC_{50}=2.9μM), the CLL cell line MEC-1 (LC_{50}=0.14μM) and primary CLL B cells derived from eight patients (LC_{50}=0.23μM). In all cases, this was associated with the selective depletion of RelA/p65 in a proteasome-dependent manner. It is noteworthy that the cytotoxicity of **15d** was two logs lower in non-malignant B- and T-lymphocytes derived from healthy volunteers and was five-fold lower in RPMI-8226 cells, which possess very low levels of CRBN protein expression.

The proteasome-recruitment mechanism of **15d** was confirmed by the reversal of RelA/p65 depletion when cells were co-treated with the proteasome inhibitor, MG-132. Furthermore, a FRET-melting assay confirmed that this compound did not interact with DNA, which was in contrast with the strong DNA interaction shown by its constituent PBD, **20d**. Hence, the cytotoxicity of **15d** appeared to be predominately driven by proteasome-dependent RelA/p65 degradation. Further screening of the small library and comparison with simulated modelling results implied that PROTAC potency may be partially related to the binding affinity of the POI ligand, while it was also reliant on ternary complex formation as demonstrated by the reduced toxicity and RelA/p65 degradation in the presence of MG-132 and reduced cytotoxicity in RPMI-8226 cells which have low cereblon expression. It is worthy of note that **15d** was not able to abolish RelA/p65 expression, which suggests that further PROTAC optimisation may be possible. Despite the incomplete target degradation observed in our studies, the work presented here demonstrates, for the first time, that it is possible to produce a PROTAC with the ability to

View Article Online
DOI: 10.1039/D5MD00316D

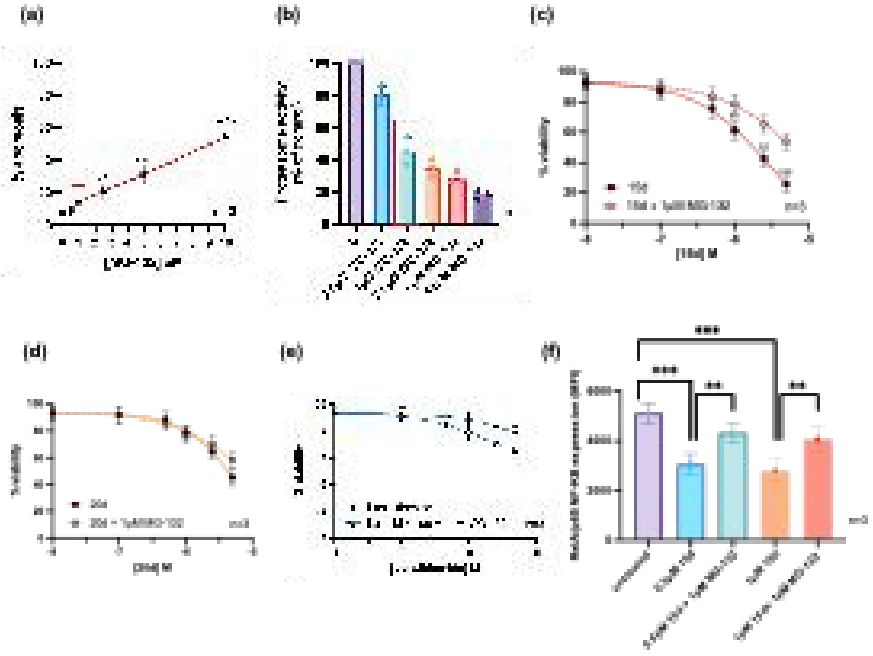

Figure 7. The effects of the proteasome inhibitor, MG-132, in the MDA-MB-231 cell line. (a) MG-132 induced dose-dependent cytotoxicity which was (b) associated with a dose-inhibition of proteasomal activity. A dose of 1μM MG-132 did cause a significant increase in cytotoxicity but induced a >50% reduction in proteasome activity. All experiments were performed in triplicate and statistical significance was determined using the Kruskal-Wallis test with Dunn's multiple comparison post hoc. ** p<0.01, *** p<0.001, ****p<0.0001. (c) Overlaid dose-response curves of MDA-MB-231 cells treated with **15d** with and without the addition of the proteasome inhibitor, MG-132. (d) **20d** (e) lenalidomide. The cytotoxic effect of **15d** was significantly reduced by co-treatment with 1μM MG-132. This was not the case for **20d** or lenalidomide. All experiments were performed in triplicate and statistical significance was determined using the Kruskal-Wallis test with Dunn's multiple comparison *post hoc* correction. *** p<0.001. (f) **15d** mediated depletion of RelA/p65 expression in MDA-MB-231 cells was dependent on proteasome activity. Experiments were performed in triplicate and statistical significance was determined using the Kruskal-Wallis test with Dunn's multiple comparison *post hoc* correction. ** p<0.01, *** p<0.001.

preferentially degrade a single NF-κB subunit, RelA/p65. As such, this may represent an important step towards unlocking the potential of NF-κB as a therapeutic target. In particular, the generation of a PROTAC with the ability to selectively degrade RelA/p65 may open the door to more effective and better tolerated treatments for human pathologies that are associated with RelA/p65 overexpression, including a range of cancers and autoimmune disorders.

EXPERIMENTAL SECTION

Molecular Docking. Protein data file was accessed from PBD data bank (p65 protein data: 1VKX), all compound ligands were prepared and generated via either Chem 3D or Avogadro. All compounds were calculated and performed with energy minimization via MMFF94. For p65-targeting ligands, the molecular docking was performed by Vina molecular docking programme using VEGA-ZZ modelling software. The parameters were set as X: -11.3, Y: 40.4, Z: 76.7; box: 30, 30, 30; exhaustiveness: 20; binding mode: 16. All docking results were visualised via Discovery Studio. The result was visualised via PyMOL.

Chemistry Materials and Methods. All synthetic chemicals, building blocks, and solvents were purchased from Fluorochem, Sigma-Aldrich, and Thermo-Fisher Scientific. All reactions monitored via thin-layer chromatography (TLC) were performed by using Supelco TLC silica gel 60 F_{254} aluminium plates. The TLC plates were visualised using a UV lamp at 254 nm. Purification through flash column chromatography was performed in glass column with silica gel as the stationary phase (230-400 mesh, 60 Å). Preparative HPLC was also used for purifying some products. An Agilent 1260 Preparative LC system was applied using H_2O (solvent A) and acetonitrile (solvent B) as the mobile phase with a Monolithic C_{18} 50 × 4.6 mm LC column (Phenomenex) as the stationary phase. Method A, B, C, and D were used for purification (Flow rate:20 ml/min). Formic acid was added (0.1%) in both solvent A and B to maintain an acidic mobile phase condition.

Method A. The gradient was initially kept at 60% solvent A and 40% solvent B, while it was ramped up to 60% B over 2 min. Solvent B was then increased to 70% over 2 min, which was further ramped up to 80% over 2.5 min. The solvent was reached to 90% B over 0.5 min and kept for 2.5 min, which was then returned to 40% B over 1.5 min.

View Article Online
DOI: 10.1039/D5MD00316D

Method B. The gradient was initially started from 90% A and 10% B and kept for 1 min, and then ramped up to 20% B over 1.5 min. B was then increased to 30% over 2 min, followed by ramping up to 40% B over 2 min. Subsequently, B was raised to 70% within 0.5 min, and then B was increased to 85% over 1 min, and then ramped up to 90% over 1 min. the solvent was finally returned to 10% B over 1 min.

Method C. The gradient was initially started from 90% A with 10% B that is kept for 1 min, and solvent B was increased to 30% over 1.5 min. B was subsequently increased to 50% over 3.5 min, and then raised to 90% over 2 min and kept for 1 min. The gradient was finally reduced to 10% B over 1 min.

Method D. The gradient was initially started from 90% A with 10% B that is kept for 1 min, and solvent B was increased to 50% over 5 min. The gradient was subsequently raised to 90% B over 2 min, and it was kept for 1 min. Solvent B was finally returned to 10% over 1 min.

High-performance liquid chromatography-tandem mass spectrometry (LCMS) was applied for monitoring reaction and characterizing products. The product analysis was carried out using an Agilent 1260 separating system using H_2O (solvent A) and acetonitrile (solvent B) as the mobile phase, while Monolithic C_{18} 50 × 4.6 mm LC column (Phenomenex) worked as stationary phase. Method E (10 min) and Method F (5 min) were used for analysis (Flow rate: 0.5 mL/min; inject volume: 200 µL), while samples were split and passed through an Agilent 6120 quadrupole mass spectrometer. Formic acid was added (0.1%) in both solvent A and B to maintain an acid mobile phase condition.

Method E (10 min run). Solvent A (95%) with Solvent B (5%) was maintained for 2 mins, and then ramped up to 50% Solvent B in 3 mins. The gradient was retained for 1 min and then Solvent B was increased to 95% in 1.5 min. Solvent B was finally returned to 5% in 1.5 min and maintained for 1 min.

Method F (5 min run). Solvent A (95%) with solvent B (5%) was ramped up to 90% in 3 min, while solvent B was then ramped up to 95% within 0.5 min. The solvent gradient was kept for 1 min, and then solvent B was reduced to 5% within 0.5 min.

tert-butyl 6-((2-(2,6-dioxopiperidin-3-yl)-1-oxoisoindolin-4-yl) amino) hexanoate (**1, JP-163-03**). lenalidomide (0.800 g, 3.09 mmol, 1 eq) was dissolved in NMP (3 mL), added with tert-butyl 6-bromo hexanete (1.010 g, 4.02 mmol, 1.3 eq) and DIPEA (1.62 mL, 9.27 mmol, 3 eq). The mixture was stirred at 130°C. After checking the progress of the reaction was finished, the mixture was quenched in 50× volume of water, and it was extracted with 3 × 30 mL EA. The organic phase was collected and washed with 3 × 30 mL water, brine, and dried over $MgSO_4$. The crude was purified in C_{18} preparative column chromatography (Method A), and 1.04 g product was obtained after evaporation (Yield: 78.3%)[25]. ^{1}H NMR (400 MHz, DMSO-d6): δ 1.38 (s, 11H), δ 1.50-1.61 (m, 4H), δ 2.02-2.08 (m, 1H), δ 2.19 (t, 2H, *J* = 7.24 Hz), δ 2.24-2.38 (m, 1H), δ 2.60-2.64 (m, 1H), δ 2.88-2.97 (m, 1H), δ 3.09-3.14 (q, 2H, *J* = 6.37 Hz), δ 4.10-4.25 (q, 2H, *J* = 19.01 Hz), δ 5.09-5.13 (dd, 1H, *J* = 5.03, 13.22 Hz), δ 5.52-5.55 (t, 1H, *J* = 5.24 Hz), δ 6.73-6.75 (d, 1H, *J* = 8.03 Hz), δ 6.92-6.93 (d, 1H, *J* = 7.38 Hz), δ 7.26-7.30 (t, 1H, *J* = 7.70 Hz), δ 10.99 (s, 1H). ^{13}C NMR (100 MHz, DMSO-d6): δ 23.32, 24.94, 26.48, 28.24, 28.66, 31.72, 35.22, 43.01, 46.18, 51.96, 79.84, 110.40, 112.19, 126.94, 129.67, 132.52, 144.22, 169.36, 171.69, 172.72, 173.34. LCMS-ESI (m/z): $C_{23}H_{31}N_3O_5$ (429.52) [M-H$^+$] 428.2; retention time 7.70 min (Method E).

6-((2-(2,6-dioxopiperidin-3-yl)-1-oxoisoindolin-4-yl) amino) hexanoic acid (**2, JP-164-05**) 1.0 g **1** was suspended in 4 ml DCM, while 2 ml TFA was added dropwise in the suspension. The suspension was immediately dissolved and was left stirring for another 2 h. After the checking of completion of the reaction, the mixture was evaporated using a rotary evaporator and dissolved in water, transferred to a vial and freeze dried to obtain the product without further purification[25]. ^{1}H NMR (400 MHz, DMSO-d6): δ 1.36-1.42 (m, 2H), δ 1.51-1.61 (m, 4H), δ 2.03-2.05 (m, 1H), δ 2.20-2.24 (t, 2H, *J* = 7.28 Hz), δ 2.29-2.33 (m, 1H), δ 2.60-2.65 (m, 1H), δ 2.90-2.93 (m, 1H), δ 3.11-3.14 (t, 2H, *J* = 6.98 Hz), δ 4.13-4.27 (q, 2H, *J* = 19.40 Hz), δ 5.10-5.14 (dd, 1H, *J* = 5.04, 13.27 Hz), δ 6.77-6.79 (d, 1H, *J* = 8.05 Hz), δ 6.95-6.97 (d, 1H, *J* = 7.42 Hz), δ 7.28-7.32 (t, 1H, *J* = 7.71 Hz), δ 11.01 (s, 1H). ^{13}C NMR (100 MHz, DMSO-d6): δ 23.28, 24.81, 26.64, 28.62, 31.71, 34.12, 43.32, 46.18, 51.97, 110.89, 112.72, 127.25, 129.71, 132.58, 143.79, 169.29, 171.70, 173.36, 174.92. LCMS-ESI (m/z): $C_{19}H_{23}N_3O_5$ (373.41) [M+H$^+$] 374.1; retention time 5.65 min (Method E); purity 98.47%

Methyl (S)-4-(5-amino-4-(2-(hydroxymethyl)pyrrolidine-1-carbonyl)-2-methoxyphenoxy)butanoate (**4, JP-179-02**) Methyl (S)-4-(4-(2-(hydroxymethyl)pyrrolidine-1-carbonyl)-2-methoxy-5-nitrophenoxy)butanoate (**3**, **MMH-165-31**, 1.440 g, 3.63 mmol, 1 eq) was dissolved in 10 mL EA/EtOH solvent mixture (EA/EtOH = 5/5). ammonium formate (0.458 g, 7.26 mmol, 2 eq) and 10% Pd/C were added to the mixture and stirred in a Parr hydrogenator at 40 Psi for 2 h. After checking the finishing of the reaction in LCMS, the mixture was filtered in Celite and washed with EtOH. The collected EtOH solution was evaporated and dried to gain 1.58 g product, which was then directly used for the next step[12]. ^{1}H NMR (400 MHz, $CDCl_3$): δ 1.72-2.01 (m, 3H), δ 2.14-2.23 (m, 3H), δ 2.49-2.61 (t, 5H, *J* = 7.13 Hz), δ 3.11-3.18 (t, 2H, *J* = 6.52 Hz), δ 3.70 (s, 1H), δ 3.97 (s, 3H), δ 4.13-4.16 (t, 2H, *J* = 6.23 Hz), δ 4.40 (m, 1H), δ 6.80 (s, 1H), δ 7.70 (s, 1H). ^{13}C NMR (100 MHz, $CDCl_3$): δ 24.20-24.43, 28.48, 30.30, 49.55, 50.86, 51.77, 56.64-56.73, 61.59, 68.40, 108.39, 109.18, 127.82, 137.10, 148.47, 154.86, 173.25. LCMS-ESI (Method E) (m/z): $C_{18}H_{24}N_2O_8$ (396.4) [M+H$^+$] 397.1; retention time 6.31 min.

Methyl (S)-4-(5-(((allyloxy)carbonyl)amino)-4-(2-(hydroxymethyl)pyrrolidine-1-carbonyl)-2-methoxyphenoxy)butanoate **(5, JP-179-04)** Allyl chloroformate (0.210 g, 1.74 mmol, 1.1 eq) in 14 mL anhydrous DCM was added dropwise to a solution of **4** (0.637 g, 2.18 mmol, 1 eq) dissolved in 19 mL anhydrous DCM and 0.32 mL pyrimidine at -10°C. The mixture was then allowed to stir at room temperature for another 2 h. Once the reaction was finished, the mixture was washed with $CuSO_4$ (32 mL), H_2O (32 mL), sat. $NaHCO_3$ (32 mL), and brine (32 mL), then dried over $MgSO_4$. The crude was evaporated and purified via flash column chromatography (0-80% EA in Hexane), gaining 0.373 g product (Yield%: 47.62%)[12]. *Rf*=0.32 (TLC: Hex/EA = 2/8). ^{1}H NMR (400 MHz, $CDCl_3$): δ 1.64-1.66 (m, 2H), δ 1.79-1.91 (m, 1H), δ 2.05-2.18 (m, 3H), δ 2.41-2.56 (m, 2H), δ 2.97 (s, 2H), δ 3.42-3.57 (m, 2H), δ 3.62 (s, 3H), δ 3.76 (s, 3H), δ 3.99-4.12 (m, 3H), δ 4.20-4.44 (m, 1H), δ 4.56-4.57 (d, 2H, *J* = 5.60 Hz), δ 5.17-5.19 (d, 1H, *J* = 10.41 Hz), δ 5.26-5.31 (d, 1H, *J* = 17.22 Hz), δ 5.86-5.90 (m,

View Article Online
DOI: 10.1039/D5MD00316D

1H), δ 6.77 (s, 1H), δ 7.20 (s, 1H), δ 7.66 (s, 1H). LCMS-ESI (Method E) (m/z): $C_{22}H_{30}N_2O_8$ (450.49) [M+H$^+$] 451.2; retention time 6.66 min.

Allyl 11-hydroxy-7-methoxy-8-(4-methoxy-4-oxobutoxy)-5-oxo-2,3,11,11a-tetrahydro-1H-benzo[e]pyrrolo[1,2-a][1,4]diazepine-10(5H)-carboxylate **(6, JP-179-05)** TEMPO (0.099 g, 0.63 mmol, 1 eq) was added to the solution of **5** (2.841 g, 6.31 mmol, 10 eq) and BAIB (3.557 g, 11.04 mmol, 12 eq) dissolved in 145.1 mL DCM, stirred for 6 h. Once the reaction was finished, the mixture was quenched and washed by 65 mL sat. sodium metabisulfite, 65 mL sat. $NaHCO_3$, 65 mL water, and 65 mL brine. The crude was dried over $MgSO_4$ and purified with flash column chromatography (0-80% EA in hexane). *Rf*=0.16 (TLC: EA/Hexane = 7/3). 1.90 g product was obtained (Yield: 67.2%)[12]. ^{1}H NMR (400 MHz, $CDCl_3$): δ 1.88-2.00 (m, 2H), δ 2.02-2.12 (m, 4H), δ 2.47 (t, 2H, *J* = 7.18 Hz), δ 3.36-3.46 (m, 1H), δ 3.46-3.55 (m, 1H), δ 3.59-3.67 (m, 4H), δ 3.83 (s, 3H), δ 3.93-4.03 (m, 2H), δ 4.37-4.40 (m, 1H), δ 4.59-4.63 (dd, 1H, *J* = 5.45, 13.28 Hz), δ 5.03-5.15 (d, 2H, *J* = 12.84 Hz), δ 5.54-5.56 (d, 1H, *J* = 9.88 Hz), δ 5.72-5.74 (m, 1H), δ 6.61 (s, 1H), δ 7.16 (s, 1H), δ 7.20 (s, 1H). LCMS-ESI (Method E) (m/z): $C_{22}H_{28}N_2O_8$ (448.47) [M+H$^+$] 449.2; retention time 5.97 min.

Allyl 7-methoxy-8-(4-methoxy-4-oxobutoxy)-5-oxo-11-((tetrahydro-2H-pyran-2-yl)oxy)-2,3,11,11a-tetrahydro-1H-benzo[e]pyrrolo[1,2-a][1,4]diazepine-10(5H)-carboxylate **(7, JP-179-06) 6** (0.394 g, 0.88 mmol) was dissolved in 6 mL EA added with 0.8 mL DHP (8.78 mmol) and 0.004 g PTSA (0.021 mmol), stirring for 2 h. After checking the reaction was completed, the crude was diluted in 6 mL EA and washed with 6 mL $NaHCO_3$, 6 mL brine. The organic phase was dried over $MgSO_4$ and evaporated. The received oil was then purified via flash column chromatography (0-80% EA in hexane). *Rf*=0.22 (TLC: EA/Hexane = 5/5). The product was obtained after evaporation in rotary evaporator and drying in the high vac (Yield: 90.1%)[12]. ^{1}H NMR (400 MHz, $CDCl_3$): δ 1.32-1.83 (m, 12H), δ 1.86-2.15 (m, 13H), δ 2.45-2.49 (t, 4H, *J* = 7.10 Hz), δ 3.37-3.55 (m, 5H), δ 3.61 (s, 7H), δ 3.81 (s, 7H), δ 3.92-4.03 (m, 4H), δ 4.25-4.43 (m, 2H), δ 4.49-4.63 (m, 2H), δ 4.95-5.12 (m, 4H), δ 5.65-5.73 (m, 1H), δ 5.78-5.86 (m, 1H), δ 6.53 (s, 1H), δ 6.80 (s, 1H), δ 7.13-7.20 (m, 2H). LCMS-ESI (Method E) (m/z): $C_{27}H_{36}N_2O_9$ (532.59) [M+H$^+$] 533.2; retention time 7.62 min.

4-((10-((allyloxy)carbonyl)-7-methoxy-5-oxo-11-((tetrahydro-2H-pyran-2-yl)oxy)-2,3,5,10,11,11a-hexahydro-1H-benzo[e]pyrrolo[1,2-a][1,4]diazepin-8-yl)oxy)butanoic acid **(8, JP-179-07) 7** (0.586 g) was dissolved in 6 mL dioxane, while 3.3 mL 2M NaOH was added to the mixture, leaving the system at room temperature to stir for 2 h. Once checked the completion of the reaction, the mixture was evaporated and dissolved in 30 mL water. 1M citric acid was titrated till pH = 3-4, and then the water layer was extracted with EA (2×20 mL). The extracted EA layer was then collected and washed with brine (20 mL), dried over $MgSO_4$. 0.528 g product was achieved after evaporation and drying (92.5%)[12]. ^{1}H NMR (400 MHz, $CDCl_3$): δ 1.35-1.61 (m, 8H), δ 1.64-1.88 (m, 4H), δ 1.88-1.97 (m, 4H), δ 2.01-2.19 (m, 8H), δ 2.43-2.58 (m, 4H), δ 3.34-3.75 (m, 8H), δ 3.84 (s, 7H), δ 3.98-4.08 (m, 4H), δ 4.26-4.43 (m, 2H), δ 4.48-4.66 (m, 2H), δ 4.86-5.11 (m, 4H), δ 5.54-5,75 (m, 2H), δ 6.51 (s, 1H), δ 6.67 (s, 1H), δ 7.15-7.20 (m, 2H). ^{13}C NMR (100 MHz, $CDCl_3$): δ 14.19, 19.72, 21.04, 23.06, 23.94, 24.05, 25.26, 25.44, 28.70, 30.10-30.19, 30.68, 30.93, 46.44, 56.13, 60.09, 60.42, 62.91, 66.88, 67.82, 86.01, 94.65, 110.82, 114.11-114.55, 125.89, 167.13, 177.33. LCMS-ESI (Method E) (m/z): $C_{26}H_{34}N_2O_9$ (518.56) [M+H$^+$] 519.2; retention time 6.96 min.

Tert-butyl (2-fluoro-4-nitrophenyl) carbamate (**10a, JP-175-P1**) 2-fluoro-4-nitroaniline (**9a**, 0.100g, 0.641 mmol, 1 eq) was suspended in 3 mL DCM with TEA (0.13 mL, 0.962 mmol, 1 eq) and DMAP (0.009 g, 0.077 mmol, 0.03 eq). di-tert-butyl decarbonate (0.147 g, 0.673 mmol, 1.1 eq) was added to the system, stirring it at r.t for 16 h. Once check the finishing of the reaction, the mixture was diluted in 4 mL DCM and washed with ice-cooled 5% citric acid (4×3 mL) and dried over Na_2SO_4. The dried crude was then purified using flash column chromatography (0-5% EA in hexane). *Rf*=0.41 (TLC: Hexane/ EA = 9/1). 0.092 g product was achieved (Yield: 56.2%). ^{1}H NMR (400 MHz, $CDCl_3$): δ 1.54 (s,9H), δ 6.99 (s, 1H), δ 7.95-7.99 (dd, 1H, *J* = 2.49, 10.91 Hz), δ 8.04-8.06 (m, 1H), δ 8.34-8.38 (t, 1H, *J* = 8.52 Hz). LCMS-ESI (Method E) (m/z): $C_{11}H_{13}FN_2O_4$ (256.23) [M-H$^+$] 255.1; retention time 8.28 min.

Tert-butyl (4-amino-2-fluorophenyl) carbamate (**11a, JP-175-P2**) **10a** (0.300 g, 1.17 mmol, 1 eq) was dissolved in EA/EtOH solvent mixture (EA/ EtOH = 2/3), while ammonium formate (0.148 g, 2.34 mmol, 2 eq) and 10% Pd/C (0.030 g) was added to the system. Mixture was reacted in hydrogenator at 40 Psi overnight. The product was filtered in Celite and washed with EtOH. The product was evaporated without further purification, gaining 0.118 g product (Yield: 44.5%). *Rf*=0.86 (TLC: 100% EA). ^{1}H NMR (400 MHz, DMSO-d6): δ 1.41 (s, 9H), δ 5.21 (s, 2H), δ 6.30 (m, 2H), δ 6.95 (s, 1H), δ 8.27 (s, 1H). ^{13}C NMR (100 MHz, DMSO-d6): δ 28.59, 39.36-40.61, 78.81, 100.73-100.96, 109.68-109.70, 114.00-114.12, 128.36, 148.27-148.37, 154.45, 156.16, 158.57. LCMS-ESI (Method E) (m/z): $C_{11}H_{15}FN_2O_2$ (226.25) [M+H$^+$] 227.1; retention time 5.77 min.

Tert-butyl (4-(6-((2-(2,6-dioxopiperidin-3-yl)-1-oxoisoindolin-4-yl) amino) hexanamido)-2-fluorophenyl) carbamate (**12a, JP-175-P3**) **2** (0.080 g, 0.214 mmol, 1 eq) was dissolved in 5 mL DMF added with DMAP (0.052 g, 0.428 mmol, 2 eq) and EDC (0.103 g, 0.535 mmol, 2.5 eq). The mixture was stirred for 30 mins and then added **11a** (0.073 g, 0.321 mmol, 1.2 eq). The mixture was quenched with 50 mL water, and it was then worked up with 3 × 20 mL EA. The organic layer was collected and washed with 3 × 50 mL water, 50 mL brine, and dried over $MgSO_4$. The dried crude was purified using flash column chromatography (0-70% EA in Hexane). *Rf*=0.06 (TLC: EA/Hexane = 8/2). 0.034 g product was achieved (Yield: 27.6%). ^{1}H NMR (400 MHz, MeOD-d4): δ 1.30 (s, 2H), δ 1.53 (s, 9H), δ 1.69-1.80 (m, 4H), δ 2.15-2.21 (m, 1H), δ 2.38-2.41 (t, 2H, *J* = 7.44 Hz), δ 2.44-2.52 (m, 1H), δ 2.77-2.82 (m, 1H), δ 2.88-2.98 (m, 1H), δ 3.25-3.28 (t, 2H, *J* = 7.09 Hz), δ 4.28 (s, 2H), δ 5.13-5.17 (dd, 1H, *J* = 5.80, 13.26 Hz), δ 6.84-6.86 (d, 1H, *J* = 7.94 Hz), δ 7.07-7.09 (d, 1H, *J* = 7.94 Hz), δ 7.14-7.16 (d, 1H, *J* = 8.83 Hz), δ 7.31-7.35 (t, 1H, *J* = 7.50 Hz), δ 7.57-7.64 (m, 2H). ^{13}C NMR (100 MHz, MeOD-d4): δ 22.85, 25.06, 26.31, 27.22, 28.43, 29.34, 29.48, 30.99, 36.34, 42.73, 46.96-48.23, 52.16, 107.16, 110.50, 112.46, 129.19, 143.70, 170.89, 173.30. LCMS-ESI (Method E) (m/z): $C_{30}H_{36}FN_5O_6$ (581.65) [M+H$^+$] 582.2; retention time 7.47 min.

N-(4-amino-3-fluorophenyl)-6-((2-(2,6-dioxopiperidin-3-yl)-1-oxoisoindolin-4-yl) amino) hexanamide (**13a, JP-175-P4**) **12a** (0.060 g, 0.103 mmol, 1 eq) was dissolved in 4 mL DCM, added with 2 mL TFA. The solvent was stirred for 1 h. After checking the

View Article Online
DOI: 10.1039/D5MD00316D

reaction was completed, the product was evaporated and directly used for the next step without further purification. ^{1}H NMR (400 MHz, MeOD-d4): δ 1.34-1.44 (m, 2H), δ 1.55-1.69 (m, 4H), δ 2.03-2.11 (m, 1H), δ2.23-2.41 (m, 4H), δ 2.66-2.70 (m, 1H), δ 2.77-2.86 (m, 1H), δ 3.14-3.18 (t, 2H, *J* = 7.20 Hz), δ 4.17-4.18 (d, 2H, *J* = 4.59 Hz), δ 5.02-5.06 (dd, 1H, *J* = 5.32, 12.92 Hz), δ 6.75-6.77 (d, 1H, *J* = 8.12 Hz), δ 6.97-6.99 (d, 1H, *J* = 7.17 Hz), δ 7.16-7.23 (m, 3H), δ 7.61-7.64 (d, 1H, *J* = 13.38 Hz). ^{13}C NMR (100 MHz, MeOD-d4): δ 22.84, 24.90, 26.22, 28.32, 29.33, 30.97, 36.30, 42.98, 45.92, 46.96-48.23, 52.17, 107.65, 110.99, 112.96, 115.76, 126.92, 129.21, 131.62, 143.23, 170.90-170.01, 173.27. LCMS-ESI (Method E) (m/z): $C_{25}H_{28}FN_5O_4$ (481.53) [M+H$^+$] 482.2; retention time 5.87 min.

Allyl 8-(4-((4-(6-((2-(2,6-dioxopiperidin-3-yl)-1-oxoisoindolin-4-yl)amino)hexanamido)-2-fluorophenyl)amino)-4-oxobutoxy)-7-methoxy-5-oxo-11-((tetrahydro-2H-pyran-2-yl)oxy)-2,3,11,11a-tetrahydro-1H-benzo[e]pyrrolo[1,2-a][1,4]diazepine-10(5H)-carboxylate (**14a, JP-175-P5**) **5** (0.040 g, 0.077 mmol, 1 eq) was dissolved in 3 mL DMF, added with DMAP (0.019 g, 0.154 mmol, 2 eq) and EDC (0.037 g, 0.193 mmol, 2.5 eq), the mixture was stirred for 30 min then added **13a** (0.044 g, 0.092 mmol, 1.2 eq), stirring overnight. After confirming the reaction was finished via TLC, the product was quenched with 10× volume of water, and it was worked up with 3 × 30 mL EA. The organic phase was combined and washed with 50 mL water, 50 mL brine, and subsequently dried over $MgSO_4$. The crude was purified using flash column chromatography (0-5% MeOH in EA). *Rf*=0.42 (TLC: EA/MeOH = 9/1) 0.034 g product was gained (Yield: 44.3%). ^{1}H NMR (400 MHz, MeOD-d4): δ 1.46-1.58 (m, 6H), δ 1.67-1,79 (m, 6H), δ 1.98-2.07 (m, 3H), δ 2.09-2.26 (m, 5H), δ 2.35-2.47 (m, 3H), δ 2.59-2.68 (m, 2H), δ 2.73-2.82 (m, 1H), δ 2.84-2.99 (m, 1H), δ 3.23-3.26 (t, 2H, *J* = 6.80 Hz), δ 3.44-3.66 (m, 5H), δ 3.87-3.93 (s, 3H), δ 4.07-4.15 (m, 2H), δ 4.26 (d, 2H, *J*= 2.38 Hz), δ 4.40-4.63 (m, 2H), δ 5.00-5.16 (m, 3H), δ 5.73-5.82 (m, 1H), δ 5.87-5.89 (d, 1H, *J* = 9.48 Hz), δ 6.82-6.84 (d,1H, *J* = 8.18 Hz), δ 6.96-6.97 (d, 1H, *J* = 4.54 Hz), δ 7.05-7.07 (d, 1H, *J* = 7.50 Hz), δ 7.14-7.20 (m, 2H), δ 7.29-7.33 (t, 1H, *J* = 7.75 Hz), δ 7.60-7.63 (d, 1H, *J* = 12.86 Hz), δ 7.72-7.77 (t, 1H, *J* = 8.57 Hz). LCMS-ESI (Method E) (m/z): $C_{51}H_{60}FN_7O_{12}$ (982.08) [M$^+$] 982.5; retention time 7.41 min.

6-((2-(2,6-dioxopiperidin-3-yl)-1-oxoisoindolin-4-yl) amino)-N-(3-fluoro-4-(4-(((S)-7-methoxy-5-oxo-2,3,5,11a-tetrahydro-1H-benzo[e]pyrrolo[1,2-a][1,4]diazepin-8-yl)oxy)butanamido)phenyl)hexanamide (**15a, JP-175-P6**) **14a** (0.097 g, 0.099 mmol, 1 eq) was dissolved in 5 mL DCM, added with palladium tetrakis[triphenylphosphine] (0.0057 g, 0.005 mmol, 0.05 eq), triphenylphosphine (0.0065 g, 0.025 mmol, 0.25 eq), and pyrrolidine (0.01 mL, 0.119 mmol, 0.25 eq). The mixture was stirred at room temperature for 2 h. The mixture was evaporated and dried, which was purified using flash column chromatography (0-20% MeOH in EA). *Rf*=0.08 (TLC: EA/MeOH = 8/2). 0.093 g product was retrieved (Yield > 99.9%). ^{1}H NMR (400 MHz, DMSO-d6): δ 1.59-1.70 (m, 2H), δ 1.60-1.70 (m, 4H), δ 1.87-1.94 (m, 2H), δ 2.02-2.09 (m, 5H), δ 2.18-2.21 (m, 2H), δ 2.32-2.37 (t, 2H, *J* = 7.18 Hz), δ 3.06-3.15 (m, 5H), δ 3.46-3.52 (m, 2H), δ 3.55-3.59 (m, 1H), δ 3.63-3.66 (m, 3H), δ 3.91-4.04 (m, 2H), δ 4.18-4.28 (m, 1H), δ 4.42-4.51 (m, 1H), δ 4.65-4.83 (m, 1H), δ 5.69 (s, 1H), δ 6.41 (s, 1H), δ 6.69-6.71 (d, 1H, *J* = 8.05 Hz), δ 6.87-6.89 (d, 1H, *J* = 7.38 Hz), δ 7.15 (s, 1H), δ 7.23-7.27 (m, 2H), δ 7.34 (s, 1H), δ 7.56 (s, 1H), δ 7.63-7.67 (m, 1H), δ 7.78-7.79 (d, 1H, *J* = 4.41 Hz), δ 9.70-9.71 (d, 1H, *J* = 4.09 Hz), δ 10.29 (s, 1H). ^{13}C NMR (100 MHz, DMSO-d6): δ 22.87, 23.16-23.29, 24.13-24.32, 25.09, 25.42-25.64, 25.98, 26.84, 28.78, 29.29, 30.70, 31.17-31.49, 32.46, 36.82, 43.09, 44.78, 45.69, 46.11-46.26, 46.84, 49.04, 52.66, 53.88-54.22, 56.09-56.35, 58.57, 67.72, 106.54-106.78, 110.10-110.63, 111.64, 114.84-115.40, 120.26-121.06, 125.58, 127.40, 129.37, 132.74, 139.83-141.06, 144.13, 147.40, 152.00, 155.49, 163.84, 164.71, 165.31, 169.39-169.80, 171.31-171.95, 172.92. LCMS-ESI (Method E) (m/z): retention time at 6.2 min, purity 97.07%. LCMS-ESI (Method F) (m/z): retention time at 2.78 min, purity > 98.5%. HRMS-ESI-ESI: $C_{42}H_{46}FN_7O_8$ (795.35) [M+H$^+$] calculated for 796.3465; found 796.3438; error -3.35 ppm.

6-((2-(2,6-dioxopiperidin-3-yl)-1-oxoisoindolin-4-yl)amino)-N-(4-(4-(((S)-7-methoxy-5-oxo-2,3,5,11a-tetrahydro-1H-benzo[e]pyrrolo[1,2-a][1,4]diazepin-8-yl)oxy)butanamido)phenyl)hexanamide (**15d, JP-163-16**) **2** (0.053 g, 0.143 mmol, 1.5 eq) was dissolved in 3 mL DMF, added with DMAP (0.023 g, 0.190 mmol, 2 eq) and EDC (0.046 g, 0.238 mmol, 2.5 eq). The mixture was stirred for 30 mins and then added **MMH-165-26** (**20d**, 0.040 g, 0.095 mmol, 1 eq) and it was stirred overnight. Once finishing the reaction, the reaction was quenched with 10× volume of water, and extracted with 3 × 30 mL EA. The organic layer was collected and washed with 3 × 30 mL water and 30 mL brine, dried over $MgSO_4$. The crude was purified via C_{18} preparative column chromatography (Method C), gaining 0.004 g product (Yield: 7.4%). ^{1}H NMR (400 MHz, DMSO-d6): δ 1.39-1.45 (m, 2H), δ 1.60-1.65 (m, 4H), δ 1.80-1.99 (m, 4H), δ 2.00-2.12 (m, 4H), δ 2.16-2.25 (m, 1H), δ 2.28-2.35 (m, 3H), δ 2.60-2.64 (m, 1H), δ 2.88-2.97 (m, 1H), δ 3.11-3.16 (m, 2H), δ 3.43-3.52 (m, 2H), δ 3.56-3.62 (m, 1H), δ 3.66 (s, 3H), δ 3.93-4.03 (m, 2H), δ 4.15-4.25 (q, 2H, *J* = 19.16 Hz), δ 5.09-5.14 (dd, 1H, *J* = 5.18, 13.30 Hz), δ 5.59 (t, 1H, *J* = 5.48 Hz), δ 6.37 (s, 1H), δ 6.74-6.76 (d, 1H, *J* = 8.06 Hz), δ 6.92-6.94 (d, 1H, *J* = 7.41 Hz), δ 7.05 (s, 1H), δ 7.21-7.34 (m, 2H), δ 7.50 (s, 4H), δ 9.79 (s, 1H), δ 9.89 (s, 1H), δ 11.00 (s, 1H). ^{13}C NMR (100 MHz, DMSO-d6): δ 23.31, 24.13, 24.97, 25.49, 26.83, 28.85, 29.31, 29.44, 30.87, 31.72, 33.06, 36.80, 43.11, 46.23, 46.84, 49.07, 51.99, 53.88, 56.11, 68.32, 110.40, 110.72, 111.81, 112.25, 119.86-119.92, 120.31, 126.94, 129.68, 132.53, 134.99, 135.12, 141.08, 144.25, 147.45, 150.70, 163.82, 164.69, 169.36, 170.68, 171.32, 171.70, 173.33. LCMS-ESI (Method E) (m/z): $C_{42}H_{47}N_7O_8$ (777.88) [M+H$^+$] 778.3; retention time 6.19 min, purity > 98.5 %. LCMS-ESI (Method F) (m/z), retention time at 2.78 min, purity 95.8%. HRMS-ESI (m/z): $C_{42}H_{47}N_7O_8$ calculated [M+H$^+$] 778.35589; found 778.3549; error -1.32 ppm.

Tert-butyl (2-methyl-4-nitrophenyl) carbamate (**10b, JP-179-P1**) 2-methyl-4-nitroaniline (**9b**, 0.800g, 5.26 mmol, 1 eq) was suspended in 5 mL DCM with TEA (1.1 mL, 7.89 mmol, 1.5 eq) and DMAP (0.077 g, 0.63 mmol, 0.12 eq). di-tert-butyl decarbonate (1.205 g, 5.52 mmol, 1.05 eq) was added to the system, leaving it stirred at r.t for 16 h. Once check the finishing of the reaction, the mixture was diluted in 30 mL DCM, and washed with ice-cooled 5% citric acid (4×20 mL) and dried over $MgSO_4$. The dried crude was then purified using flash column chromatography (0-5% EA in hexane). *Rf*=0.16 (TLC: Hexane/ EA = 9/1). 0.465 g product was achieved (Yield: 35.0%). ^{1}H NMR (400 MHz, $CDCl_3$): δ 1.55 (s, 9H), δ 2.33 (s, 3H), δ 6.58 (s, 1H), δ 8.04-8.09 (m, 2H), δ 8.21-8.24 (d, 1H, *J* = 9.07 Hz). ^{13}C NMR (100 MHz, $CDCl_3$): δ 17.67, 28.23, 81.97, 118.12, 123.10, 125.44-125.65, 142.37-142.76, 151.90. LCMS-ESI

View Article Online
DOI: 10.1039/D5MD00316D

(Method E) (m/z): $C_{12}H_{16}N_2O_4$ (252.27) [M-H$^+$] 251.1; retention time 8.27 min.

Tert-butyl (4-amino-2-methylphenyl) carbamate (**11b, JP-179-P2**) **10b** (0.200 g, 0.79 mmol, 1 eq) was dissolved in EA/EtOH solvent mixture (EA/ EtOH = 2/3), while ammonium formate (0.100 g, 1.58 mmol, 2 eq) and 10% Pd/C (0.020 g) was added to the system. Mixture was reacted in hydrogenator at 40 psi overnight. The product was filtered in Celite and washed with EtOH. The product was evaporated without further purification, yielding 0.192 g product. ^{1}H NMR (400 MHz, DMSO-d6): δ 1.41 (s, 9H), δ 2.02 (s, 3H), δ 4.83 (s, 2H), δ 6.30-6.33 (dd, 1H, *J* = 2.47, 8.31 Hz), δ 6.36-6.37 (d, 1H, *J* = 2.26 Hz), δ 6.77-6.79 (d, 1H, *J* = 8.27 Hz), δ 8.06 (s, 1H). ^{13}C NMR (100 MHz, DMSO-d4): δ 18.36, 28.69, 78.28, 111.91, 115.70, 125.73, 127.65, 134.35, 146.71, 154.77. LCMS-ESI (Method E) (m/z): $C_{12}H_{18}N_2O_2$ (222.28) [M+H$^+$] 223.1; retention time 4.74 min.

Tert-butyl (4-(6-((2-(2,6-dioxopiperidin-3-yl)-1-oxoisoindolin-4-yl) amino) hexanamido)-2-methylphenyl) carbamate (**12b, JP-179-P3**) **2** (0.258 g, 0.690 mmol, 1 eq) was dissolved in 3 mL DMF added with DMAP (0.169 g, 1.38 mmol, 2 eq) and EDC (0.331 g, 1.725 mmol, 2.5 eq). The mixture was stirred for 30 mins and then added **11b** (0.184 g, 0.828 mmol, 1.2 eq). The mixture was quenched with 10× volume water, and it was then worked up with 3 × 20 mL EA. The organic layer was collected and washed with 3 × 30 mL water, 30 mL brine, and dried over $MgSO_4$. The dried crude was purified using flash column chromatography (0-90% EA in Hexane). *Rf*=0.08 (TLC: EA/Hexane = 9/1). 0.074 g product was achieved (Yield: 18.5%). ^{1}H NMR (400 MHz, DMSO-d6): δ 1.44 (m, 11H), δ 1.58-1.66 (m, 4H), δ 1.98-2.00 (m, 1H), δ 2.14 (s, 3H), δ 2.27-2.33 (m, 3H), δ 2.60-2.67 (m, 1H), δ 2.88-2.97 (m, 1H), δ 3.11-3.18 (m, 2H), δ 4.10-4.25 (q, 2H, *J* = 19.23 Hz), δ 5.09-5.13 (dd, 1H, *J* = 5.05, 13.24 Hz), δ 5.56-5.59 (t, 1H, *J* = 5.27 Hz), δ 6.74-6.76 (d, 1H, *J* = 8.05 Hz), δ 6.92-6.93 (d, 1H, *J* = 7.44 Hz), δ 7.14-7.17 (d, 1H, *J* = 8.88 Hz), δ 7.26-7.34 (m, 2H), δ 7.40 (s, 1H), δ 8.40 (s, 1H), δ 9.75 (s, 1H), δ 11.00 (s, 1H). LCMS-ESI (Method E) (m/z): $C_{31}H_{39}N_5O_6$ (577.68) [M+H$^+$] 578.3; retention time 7.34 min.

N-(4-amino-3-methylphenyl)-6-((2-(2,6-dioxopiperidin-3-yl)-1-oxoisoindolin-4-yl)amino)hexanamide (**13b, JP-179-P4**) **12b** (0.103 g, 0.178 mmol, 1 eq) was dissolved in 4 mL DCM, added with 2 mL TFA. The solvent was stirred for 1 h. After checking the reaction was completed, the product was evaporated and directly used for the next step without further purification. ^{1}H NMR (400 MHz, MeOD-d4): δ 1.48-1.54 (m, 2H), δ 1.60-1.84 (m, 4H), δ 2.14-2.19 (m, 1H), δ 2.35-2.43 (m, 5H), δ 2.45-2.60 (m, 1H), δ 2.74-2.94 (m, 2H), δ 3.22-3.26 (t, 2H, *J* = 7.00 Hz) δ 4.25-4.27 (d, 2H, *J* = 4.81 Hz), δ 5.11-5.15 (dd, 1H, *J* = 5.14, 13.29 Hz), δ 6.82-6.84 (d, 1H, *J* = 8.01 Hz), δ 7.04-7.06 (d, 1H, *J* = 7.48 Hz), δ 7.23-7.31 (m, 2H), δ 7.50-7.52 (m, 2H). ^{13}C NMR (100 MHz, MeOD-d4): δ 15.82, 22.84, 25.03, 26.28, 28.42, 29.33-29.49, 30.97, 36.36, 42.87, 45.95, 52.17, 110.69, 112.68, 118.34, 122.37, 123.06, 124.84, 126.75, 129.18, 131.57, 132.18, 143.51, 170.91, 173.27-173.32. LCMS-ESI (Method E) (m/z): $C_{26}H_{31}N_5O_4$ (477.57) [M+H$^+$] 478.2; retention time 4.97 min.

Allyl 8-(4-((4-(6-((2-(2,6-dioxopiperidin-3-yl)-1-oxoisoindolin-4-yl)amino)hexanamido)-2-methylphenyl)amino)-4-oxobutoxy)-7-methoxy-5-oxo-11-((tetrahydro-2H-pyran-2-yl)oxy)-2,3,11,11a-tetrahydro-1H-benzo[e]pyrrolo[1,2-a][1,4]diazepine-10(5H)-carboxylate (**14b, JP-179-P5**) **8** (0.090 g, 0.174 mmol, 1 eq) was dissolved in 3 mL DMF, added with DMAP (0.043 g, 0.348 mmol, 2 eq) and EDC (0.083 g, 0.435 mmol, 2.5 eq), the mixture was stirred for 30 min then added **13b** (0.100 g, 0.209 mmol, 1.2 eq), stirring overnight. After confirming the reaction was finished via TLC, the product was quenched with 10× volume of water, and it was worked up with 3 × 30 mL EA. The organic phase was combined and washed with 50 mL water, 50 mL brine, and subsequently dried over $MgSO_4$. The crude was purified using flash column chromatography (0-5% MeOH in EA). *Rf*=0.28 (TLC: EA/MeOH = 9/1). 0.075 g product was gained (Yield: 44.1%). ^{1}H NMR (400 MHz, MeOD-d4): δ 1.45-1.56 (m, 6H), δ 1.68-1.79 (m, 6H), δ 1.97-2.07 (m, 3H), δ 2.09-2.26 (m, 5H), δ 2.33-2.48 (m, 3H), δ 2.57-2.70 (m, 2H), δ 2.73-3.00 (m, 2H), δ 3.22-3.26 (t, 2H, *J* = 6.85 Hz), δ 3.41-3.72 (m, 5H), δ 3.87-3.93 (m, 3H), δ 4.06-4.19 (m, 2H), δ 4.26 (s, 2H), δ 4.38-4.62 (m, 2H), δ 5.00-5.16 (m, 3H), δ 5.73-5.82 (m, 1H), δ 5.87-5.89 (d, 1H, *J* = 9.48 Hz), δ 6.82-6.84 (d, 2H, *J* = 8.18 Hz), δ 6.96-6.97 (d, 1H, *J* = 4.54 Hz), δ 7.05-7.07 (d, 1H, *J* = 7.50 Hz), δ 7.11-7.23 (m, 2H), δ 7.29-7.33 (t, 1H, *J* = 7.77 Hz), δ 7.60-7.63 (d, 1H, *J* = 12.86 Hz), δ 7.72-7.77 (t, 1H, *J* = 8.73 Hz). LCMS-ESI (Method E) (m/z): $C_{52}H_{63}N_7O_{12}$ (978.12) [M$^+$/2] 489.7; retention time 7.32 min.

6-((2-(2,6-dioxopiperidin-3-yl)-1-oxoisoindolin-4-yl)amino)-N-(4-(4-(((S)-7-methoxy-5-oxo-2,3,5,11a-tetrahydro-1H-benzo[e]pyrrolo[1,2-a][1,4]diazepin-8-yl)oxy)butanamido)-3-methylphenyl)hexanamide (**15b, JP-179-P6**) **14b** (0.075 g, 0.077 mmol, 1 eq) was dissolved in 5 mL DCM, added with palladium tetrakis[triphenylphosphine] (0.0045 g, 0.004 mmol, 0.05 eq), triphenylphosphine (0.0050 g, 0.019 mmol, 0.25 eq), and pyrrolidine (0.008 mL, 0.092 mmol, 1.2 eq). The mixture was stirred at room temperature for 2 h. The mixture was then evaporated and dried, which was purified using flash column chromatography (0-20% MeOH in EA). *Rf*=0.38 (TLC: EA/MeOH = 8/2). 0.053 g product was retrieved (Yield: 86.9%). ^{1}H NMR (400 MHz, DMSO-d6): δ 1.36-1.48 (m, 2H), δ 1.57-1.70 (m, 4H), δ 1.84-1.98 (m, 2H), δ 1.99-2.07 (m, 3H), δ 2.12 (s, 3H), δ 2.19-2.39 (m, 5H), δ 2.49-2.52 (m, 2H), δ 2.58-2.68 (d, 1H, *J* = 16.87 Hz), δ 2.83-3.00 (m, 1H), δ 3.07-3.19 (m, 2H), δ 3.33-3.45 (m, 2H), δ 3.54-3.62 (m, 1H), δ 3.57-3.76 (m, 3H), δ 3.97-4.10 (m, 2H), δ 4.13-4.27 (m, 2H), δ 5.00-5.21 (dd, 1H, *J* = 12.80, 4.68 Hz), δ 5.57 (s, 1H), δ 6.74-6.76 (d, 1H, *J* = 7.98 Hz), δ 6.92-6.94 (d, 1H, *J* = 7.37 Hz), δ 7.23-7.30 (m, 2H), δ 7.35-7.39 (d, 2H, *J* = 8.11 Hz), δ 7.45 (s, 1H), δ 7.56 (s, 1H), δ 7.78-7.79 (d, 1H, *J* = 4.13 Hz), δ 9.28 (s, 1H), δ 9,81 (s, 1H), δ 11.00 (s, 1H). ^{13}C NMR (100 MHz, DMSO-d6): δ 14.55, 18.56, 21.22, 23.31, 24.14, 25.23, 25.50, 26.81, 28.85, 29.31, 31.72, 36.83, 43.11, 46.25, 46.84, 51.99, 53.88, 54.21, 56.10, 60.22, 68.36, 110.39, 110.70, 111.80, 112.22, 117.23, 121.18, 126.20, 126.95, 129.68, 131.92, 132.53, 132.85, 141.08, 144.25, 147.45, 150.71, 164.70, 169.37, 171.00, 171.48, 171.71, 173.35. LCMS-ESI (Method E) (m/z): $C_{43}H_{49}N_7O_8$ (791.91) 792.3; retention time 6.16 min; purity 95.66%. LCMS-ESI (Method F) (m/z): retention time at 2.73 min, purity 98.5%. HRMS-ESI (m/z): $C_{43}H_{49}N_7O_8$ (791.27) [M+H$^+$] calculated 792.3715; found 792.3703; error -1.56 ppm.

Tert-butyl (2-methoxy-4-nitrophenyl) carbamate **(10c, JP-179-P7)** 2-methoxy-4-nitroaniline (**9c**, 0.800g, 4.76 mmol, 1 eq) was suspended in 5 mL DCM with TEA (1.0 mL, 7.14 mmol, 1.5 eq) and DMAP (0.069 g, 0.57 mmol, 0.12 eq). Di-tert-butyl decarbonate (1.091 g, 5.00 mmol, 1.05 eq) was then added, leaving it stirred at r.t for 16 h. Once reaction was finished, the mixture was diluted in

View Article Online
DOI: 10.1039/D5MD00316D

30 mL DCM and washed with ice-cooled 5% citric acid (4 × 20 mL) and dried over $MgSO_4$. The dried crude was then purified using flash column chromatography (0-5% EA in hexane). *Rf*=0.22 (TLC: Hexane/ EA = 9/1). 0.764 g product was achieved (Yield: 59.7%). ^{1}H NMR (400 MHz, $CDCl_3$): δ 1.54 (s, 9H), δ 3.98 (s, 3H), δ 7.35 (s, 1H), δ 7.72 (s, 1H), δ 7.90-7.92 (dd, 1H, *J* = 2.09, 9.04 Hz), δ 8.25-8.28 (d, 1H, *J* = 9.02 Hz). ^{13}C NMR (100 MHz, $CDCl_3$): δ 28.24, 56.26, 81.71, 105.18, 116.36, 117.89, 134.66, 142.15, 146.81, 152.00. LCMS-ESI (Method E) (m/z): $C_{12}H_{16}N_2O_5$ (268.27) [M-H$^+$] 267.1; retention time 8.55 min.

Tert-butyl (4-amino-2-methoxyphenyl) carbamate (**11c, JP-179-P8**) **10c** (0.300 g, 1.118 mmol, 1 eq) was dissolved in EA/EtOH solvent mixture (EA/ EtOH = 2/3), while ammonium formate (0.141 g, 2.236 mmol, 2 eq) and 10% Pd/C was added to the system. The mixture was reacted in hydrogenator at 40 psi overnight. The product was filtered in Celite and washed with EtOH. The product was evaporated without further purification, yielding 0.267 g product. ^{1}H NMR (400 MHz, DMSO-d6): δ 1.41 (s, 9H), δ 3.68 (s, 3H), δ 4.92 (s, 2H), δ 6.07-6.09 (d, 1H, *J* = 8.37 Hz), δ 6.23 (s, 1H), δ 7.04 (s, 1H), δ 7.52 (s, 1H). ^{13}C NMR (100 MHz, DMSO-d6): δ 28.64, 55.57, 78.55, 98.25, 105.67, 116.27, 147.03, 154.18. LCMS-ESI (Method E) (m/z): $C_{12}H_{18}N_2O_3$ (238.29) [M+H$^+$] 239.1; retention time 5.04 min.

Tert-butyl (4-(6-((2-(2,6-dioxopiperidin-3-yl)-1-oxoisoindolin-4-yl) amino) hexanamido)-2-methoxyphenyl) carbamate **(12c, JP-179-P9) 2** (0.261 g, 0.699 mmol, 1 eq) was dissolved in 3 mL DMF added with DMAP (0.171 g, 1.398 mmol, 2 eq) and EDC (0.335 g, 1.748 mmol, 2.5 eq). The mixture was stirred for 30 mins and then added **11c** (0.200 g, 0.839 mmol, 1.2 eq). The mixture was quenched with 10× volume water, and it was then worked up with 3 × 20 mL EA. The organic layer was collected and washed with 3 × 30 mL water, 30 mL brine, and dried over $MgSO_4$. The dried crude was purified using flash column chromatography (0-90% EA in Hexane). *Rf*=0.08 (TLC: EA/Hexane = 9/1). 0.152 g product was achieved (Yield: 36.6%). ^{1}H NMR (400 MHz, MeOD-d4): δ 1.51 (m, 11H), δ 1.70-1.78 (m, 4H), δ 2.12-2.17 (m, 1H), δ 2.37-2.40 (m, 3H), δ 2.86-2.99 (m, 3H), δ 3.24-3.28 (t, 2H, *J* = 6.92 Hz), δ 3.84 (s, 3H), δ 4.26 (s, 2H), δ 5.10-5.14 (dd, 1H, *J* = 5.06, 13.38 Hz), δ 6.83-6.85 (d, 1H, *J* = 8.08 Hz), δ 6.94-6.96 (m, 1H), δ 7.05-7.07 (d, 1H, *J* = 7.49 Hz), δ 7.29-7.33 (t, 1H, *J* = 7.93 Hz), δ 7.39 (s, 1H), δ 7.68-7.70 (d, 1H, *J* = 7.90 Hz). LCMS-ESI (Method E) (m/z): $C_{31}H_{39}N_5O_7$ (593.68) [M+H$^+$] found 594.3; retention time 7.59 min.

N-(4-amino-3-methoxyphenyl)-6-((2-(2,6-dioxopiperidin-3-yl)-1-oxoisoindolin-4-yl) amino) hexanamide **(13c, JP-179-P10) 12c** (0.144 g, 0.242 mmol, 1 eq) was dissolved in 4 mL DCM, added with 2 mL TFA. The solvent was stirred for 1 h. After checking the reaction was completed, 0.163 g product was obtained and directly used for the next step without further purification. ^{1}H NMR (400 MHz, MeOD-d4): δ 1.48-1.55 (m, 2H), δ 1.70-1.77 (m, 4H), δ 2.15-2.18 (m, 1H), δ 2.40-2.50 (m, 3H), δ 2.75-2.99 (m, 2H), δ 3.24-3.27 (t, 2H, *J* = 7.00 Hz), δ 3.94 (s, 3H), δ 4.27-4.28 (d, 2H, *J* = 4.53 Hz), δ 5.12-5.17 (dd, 1H, *J* = 5.15, 13.35 Hz), δ 6.83-6.85 (d, 1H, *J* = 7.99 Hz), δ 7.05-7.07 (d, 1H, *J* = 7.48 Hz), δ 7.13-7.14 (d, 1H, *J* = 10.05 Hz), δ 7.24-7.32 (m, 2H), δ 7.60 (s, 1H). ^{13}C NMR (100 MHz, MeOD-d4): δ 22.86, 24.99, 26.29, 28.44, 30.97, 36.43, 42.87, 45.91, 48.44, 52.15, 53.73, 55.29, 103.59, 110.72, 111.44, 112.69, 123.42, 126.76, 129.19, 131.57, 143.47, 152.82, 170.90-171.07, 173.27-173.39. LCMS-ESI (Method E) (m/z): $C_{26}H_{31}N_5O_5$ (493.56) [M+H$^+$] 494.2; retention time 4.89 min.

Allyl 8-(4-((4-(6-((2-(2,6-dioxopiperidin-3-yl)-1-oxoisoindolin-4-yl)amino)hexanamido)-2-methoxyphenyl)amino)-4-oxobutoxy)-7-methoxy-5-oxo-11-((tetrahydro-2H-pyran-2-yl)oxy)-2,3,11,11a-tetrahydro-1H-benzo[e]pyrrolo[1,2-a][1,4]diazepine-10(5H)-carboxylate **(14c, JP-179-P11) 8** (0.090 g, 0.174 mmol, 1 eq) was dissolved in 3 mL DMF, added with DMAP (0.043 g, 0.348 mmol, 2 eq) and EDC (0.083 g, 0.435 mmol, 2.5 eq), the mixture was stirred for 30 min then added **13c** (0.100 g, 0.209 mmol, 1.2 eq), stirring overnight. After confirming the reaction was finished via TLC, the product was quenched with 10× volume of water, and it was worked up with 3 × 30 mL EA. The organic phase was combined and washed with 50 mL water, 50 mL brine, and subsequently dried over $MgSO_4$. The crude was purified using flash column chromatography (0-5% MeOH in EA). *Rf*=0.26 (TLC: EA/MeOH = 9/1). 0.116 g product was gained (Yield: 67.1%). ^{1}H NMR (400 MHz, MeOD-d4): δ 1.21-1.46 (m, 8H), δ 1.54-1.81 (m, 6H), δ 1.82-2.10 (m, 7H), δ 2.10-2.50 (m, 6H), δ 2.50-2.55 (m, 2H), δ 2.62-2.89 (m, 2H), δ 3.33-3.49 (m, 3H), δ 3.55-3.64 (m, 1H), δ 3.70-3.84 (m, 6H), δ 3.98-4.07 (m, 2H), δ 4.26-4.40 (m, 1H), δ 4.46-4.73 (m, 2H), δ 4.97-5.14 (m, 2H), δ 5.66-5.68 (d, 1H, *J* = 6.77 Hz), δ 5.79-5.81 (d, 1H, *J* = 8.96 Hz), δ 6.56-6.70 (m, 1H), δ 6.83 (m, 1H), δ 7.12-7.19 (m,2H), δ 7.33-7.63 (m, 3H), δ 7.70-7.75 (m, 1H). LCMS-ESI (Method E) (m/z): $C_{52}H_{63}N_7O_{13}$ (944.11) [M$^+$] 944.4; retention time 7.41 min.

6-((2-(2,6-dioxopiperidin-3-yl)-1-oxoisoindolin-4-yl)amino)-N-(3-methoxy-4-(4-(((S)-7-methoxy-5-oxo-2,3,5,11a-tetrahydro-1H-benzo[e]pyrrolo[1,2-a][1,4]diazepin-8-yl)oxy)butanamido)phenyl)hexanamide **(15c, JP-179-P12) 14c** (0.116 g, 0.117 mmol, 1 eq) was dissolved in 5 mL DCM, added with palladium tetrakis[triphenylphosphine] (0.0068 g, 0.006 mmol, 0.05 eq), triphenylphosphine (0.0077 g, 0.029 mmol, 0.25 eq), and pyrrolidine (0.01 mL, 0.140 mmol, 1.2 eq). The mixture was stirred at room temperature for 2 h. The mixture was then evaporated and dried in a rotary evaporator, which was purified using flash column chromatography (0-20% MeOH in EA). *Rf*=0.34 (TLC: EA/MeOH = 8/2). 0.096 g product was retrieved (Yield > 99.9%). ^{1}H NMR (400 MHz, DMSO-d6): δ 1.36-1.49 (m, 2H), δ 1.59-1.68 (m, 4H), δ 1.80-1.95 (m, 2H), δ 1.95-2.10 (m, 5H), δ 2.15-2.38 (m, 5H), δ 2.51-2.61 (m, 2H), δ 3.06-3.16 (m, 2H), δ 3.40-3.49 (m, 2H), δ 3.55-3.61 (m, 1H), δ 3.67 (s, 3H), δ 3.76 (s, 3H), δ 3.91-4.06 (m, 2H), δ 4.22-4.52 (m, 2H), δ 4.64-4.81 (dd, 1H, *J* = 10.27,4.73 Hz), δ 5.67 (s, 1H), δ 6.12 (s, 1H), δ 6.39 (s, 1H), δ 6.68-6.78 (m, 1H), δ 6.86-6.92 (m, 1H), δ 7.06-7.08 (d, 1H, *J* = 7.48 Hz), δ 7.24-7.27 (m, 2H), δ 7.46 (s, 1H), δ 7.57 (s, 1H), δ 7.73-7.75 (d, 1H, *J* = 8.35 Hz), δ 9.07 (s, 1H), δ 9.93 (s, 1H). ^{13}C NMR (100 MHz, DMSO-d6): δ 22.88, 25.25, 25.49, 26.89, 28.85, 29.54, 30.72, 30.85, 31.67, 32.74, 36.89, 43.12, 45.96, 51.78, 53.59, 54.21, 54.69, 55.92, 56.29, 56.39, 58.59, 58.86, 95.26, 103.16, 110.22, 110.93, 113.03, 115.57, 122.81, 123.31, 127.24, 129.47, 136.88, 139.82, 141.17, 144.23, 152.11, 165.29, 167.38, 171.01, 171.56, 172.42, 173.00. LCMS-ESI (Method E) (m/z): $C_{43}H_{49}N_7O_9$ (807.37) [M-H$^+$] 806.3; racemic structure peaks of the final product observed at 6.27 and 6.35 min; purity 90.63%. LCMS-ESI (Method E) (m/z): peak at 2.80 min, purity 96.2%. HRMS-ESI (m/z): $C_{43}H_{49}N_7O_9$ (807.37) [M+H$^+$] calculated 808.36645; found 808.3655; error -1.20 ppm.

View Article Online
DOI: 10.1039/D5MD00316D

Allyl (3-fluoro-4-nitrophenyl) carbamate (**17a, JP-193-09**) 3-Fluoro-4 nitroaniline (**16a**, 0.100 g, 0.641 mmol, 1 eq) was added in 2 mL THF, then added with K_2CO_3 (0.106 g, 0.769 mmol, 1.2 eq). Allyl chloroformate (0.08 mL, 0.705 mmol, 1.1 eq) was then added dropwise, and the mixture was stirred overnight. The reaction was quenched with 10 mL DCM and washed with 10 mL $CuSO_4$, 3 × 10 mL Sat. Na2CO3, and dried over Na_2SO_4. The organic layer was evaporated in a rotary evaporator and then purified in flash chromatography (0-10% EA in Hexane). *Rf*=0.58 (TLC: EA/Hexane = 2/8). Product was finally obtained 0.112 g (Yield: 72.7%). ^{1}H NMR (400 MHz, $CDCl_3$): δ 4.70-4.71 (d, 2H, *J* = 5.84 Hz), δ 5.30-5.32 (d, 1H, *J* = 10.40 Hz), δ 5.36-5.41 (dd, 1H, *J* = 1.26, 17.19 Hz), δ 5.91-6.01 (m, 1H), δ 7.06 (s, 1H), δ 7.11-7.14 (d, 1H, *J* = 9.09 Hz), δ 7.61-7.64 (d, 1H, *J* = 13.16 Hz), δ 8.05-8.09 (t, 1H, *J* = 8.66 Hz). ^{13}C NMR (100 MHz, $CDCl_3$): δ 66.77, 106.86-107.12, 113.06-113.09, 119.28, 127.46-127.48, 131.52, 144.73-144.84, 152.23, 155.62, 158.24. LCMS-ESI (Method E) (m/z): $C_{10}H_9FN_2O_4$ 240.19 [M-H$^+$] 239.0; retention time 7.66 min.

Allyl (4-amino-3-fluorophenyl) carbamate (**18a, JP-193-10**) **17a** (0.104 g, 0.431 mmol, 1 eq) was dissolved in 2 mL EtOH/H_2O solvent mixture (ratio: 3/1), added with iron powder (0.144 g, 2.586 mmol, 6 eq) and NH_4Cl (0.207 g, 3.879 mmol, 9 eq). The suspension was stirred at 80°C for 2h. Once the reaction was confirmed finished via TLC, the reaction was quenched by cooling the reaction to r.t., and the suspension was filtered via Celite. The filtered organic layer was evaporated in a rotary evaporator and redissolved in EA, washed with water, brine, and dried over $MgSO_4$. The solvent was then filtered and evaporated in a rotary evaporator, fully dried to obtain 0.096 g product and it was directly used without further purification. ^{1}H NMR (400 MHz, DMSO-d6): δ 4.56-4.69 (dt, 2H, J = 5.40, 1.38 Hz), δ 4.80 (s, 2H), δ 5.20-5.23 (dd, 1H, J = 10.46, 1.26 Hz), δ 5.31-5.36 (dd, 1H, J = 18.12, 1.40 Hz), δ 5.93-5.99 (m, 1H), δ 6.65-6.70 (m, 1H), δ 6.89-6.91 (d, 1H, J = 8.05 Hz), δ 7.16-7.19 (d, 1H, J = 12.87 Hz), δ 9.41 (s, 1H). ^{13}C NMR (100 MHz, DMSO-d6): δ 64.93, 115.52, 116.65-116.71, 117.88, 128.94, 133.91, 149.38, 151.72, 153.75. LCMS-ESI (Method E) (m/z): $C_{10}H_{11}FN_2O_2$ (211.21) [M+H$^+$] 211.1; retention time 5.10 min (Method E).

Allyl 8-(4-((4-(((allyloxy) carbonyl) amino)-2-fluorophenyl) amino)-4-oxobutoxy)-7-methoxy-5-oxo-11-((tetrahydro-2H-pyran-2-yl)oxy)-2,3,11,11a-tetrahydro-1H-benzo[e]pyrrolo[1,2-a] [1,4] diazepine-10(5H)-carboxylate (**19a, JP-193-11**) **8** (0.090 g, 0.174 mmol, 1 eq) was dissolved in 3 mL DMF, added with DMAP (0.085 g, 0.696 mmol, 4 eq) and EDC (0.166 g, 0.870 mmol, 5 eq). The mixture was stirred for 30 mins, then added **18a** to leave the reaction stirred at r.t. overnight. The reaction was quenched with 10× volume H_2O, and it was extracted with 3 × 30 mL EA, the organic layer was combined with and washed with 100 mL 1M citric acid, 100 mL water, 100 mL brine, and dried over $MgSO_4$. The organic layer was evaporated in a rotary evaporator and purified using flash column chromatography (40-80% EA in Hexane). *Rf*=0.18 (TLC: Hex/EA = 4/6). The product was collected and evaporated in a rotary evaporator, followed by drying in high vac and obtained 0.122 g (Yield: 98.4%). ^{1}H NMR (400 MHz, MeOD-d4): δ 1.46-1.65 (m, 4H), δ 1.68-1.85 (m, 2H), δ 2.03-2.10 (m, 2H), δ 2.11-2.28 (m, 4H), δ 2.51-2.75 (m, 2H), δ 3.46-3.55 (m, 2H), δ 3.56-3.70 (m, 2H), δ 3.90 (s, 3H), δ 3.93-4.01 (m, 1H), δ 4.09-4.18 (m, 3H), δ 4.42-4.75 (m, 4H), δ 5.03-5.15 (m, 2H), δ 5.24-5.27 (d, 1H, J = 10.50 Hz), δ 5.36-5,41 (dd, 1H, J = 1.10, 17.22 Hz), δ 5.79-5.81 (m, 1H), δ 5.89-5.92 (d, 1H, J = 9.39 Hz), δ 5.96-6.06 (m, 1H), δ 6.89 (s, 1H), δ 6.98-7.03 (m, 1H), δ 7.10-7.12 (d, 1H, J = 8.73 Hz), δ 7.20-7.24 (m, 1H), δ 7.46-7.49 (d, 1H, J = 12.80 Hz), δ 7.68-7.72 (t, 1H, J = 7.83 Hz). LCMS-ESI (Method E) (m/z): $C_{36}H_{43}FN_4O_{10}$ 710.76; retention time 7.78 min.

(S)-N-(4-amino-2-fluorophenyl)-4-((7-methoxy-5-oxo-2,3,5,11a-tetrahydro-1H-benzo[e]pyrrolo[1,2-a][1,4]diazepin-8-yl)oxy)butanamide (**20a, JP-193-12**) **19a** (0.106 g, 0.149 mmol, 1 eq) was dissolved 5 mL DCM, added with PPh_3 (0.0197 g, 0.075 mmol, 0.5 eq), palladium tetrakis[triphenylphosphine] (0.017 g, 0.015 mmol, 0.1 eq), and pyrrolidine (0.019 mL, 0.224 mmol, 1.5 eq). The solvent was stirred for 2 h. The reaction was quenched via evaporation in a rotary evaporator and dried in high vac. The crude was further purified using flash column chromatography (0-3% MeOH in EA). *Rf*=0.38 (TLC: EA/MeOH = 9/1) The product was collected, evaporated in a rotary evaporator, and dried in high vac. The compound was further purified via preparative column chromatography (Method D) 0.020 g product was obtained (Yield: 29.9%). ^{1}H NMR (400 MHz, DMSO-d6): δ 1.94-2.05 (m, 4H), δ 2.45-2.47 (m, 2H), δ 2.10-2.34 (m, 2H), δ 2.46 (m, 2H) δ 3.17 (s, 3H), δ 3.64-3.67 (m, 2H), δ 3.74-3.82 (m, 1H), δ 3.92 (s, 2H), δ 5.25 (s, 2H), δ 6.33-6.37 (dd, 1H, J = 15.85, 13.23 Hz), δ 6.83 (s, 1H), δ 7.06-7.12 (m, 2H), δ 7.34 (s, 1H), δ 7.77-7.79 (d, 1H, *J* = 4.19 Hz), δ 9.25 (s, 1H). ^{13}C NMR (100 MHz, DMSO-d6): δ 24.13, 25.12, 29.29, 32.25, 49.07, 53.89, 56.09, 56.30, 56.40, 100.65, 100.88, 109.70, 110.60, 111.73, 114.11, 120.25, 127.66, 141.06, 147.40, 150.67, 163.81, 164.73, 171.12. LCMS-ESI (Method E) (m/z): $C_{23}H_{26}FN_4O_4$ (440.19) [M+H$^+$] 441.1; retention time 4.49 min; purity: 85.4%. LCMS-ESI (Method F) (m/z): retention time at 3.05 min, purity 92.5%. HRMS-ESI: $C_{23}H_{25}FN_4O_4$ (440.19) [M+H$^+$] calculated 441.19326; found 441.1930; error -0.68 ppm.

Allyl (3-methyl-4-nitrophenyl) carbamate (**17b, JP-193-13**) 3-Methyl-4-nitroaniline (**16b**, 0.100 g, 0.657 mmol, 1 eq) was dissolved in 2 mL DMF, which was added with K_2CO_3 (0.109 g, 0.788 mmol, 1.2 eq) and 97% allyl chloroformate (0.11 mL, 0.723 mmol, 1.1 eq). The mixture was allowed to stir at r.t. overnight. After reaction was finished, the reaction was confirmed finished via TLC, it was quenched by 10 mL DCM, and it was washed with 10 sat. $CuSO_4$, 3 × 10 mL water, 3 × 10 mL Na_2CO_3. The organic layer was then dried over sodium sulphate, filtered, and then evaporated via rotary evaporator. The crude was purified using flash column chromatography (0-10% EA in hexane). *Rf*=0.60 (TLC: Hexane/EA = 8/2). The product was collected and evaporated in a rotary evaporator, gaining 0.130 g product after fully dried in high vac (Yield: 83.7%). ^{1}H NMR (400 MHz, $CDCl_3$): δ 2.56 (s, 3H), δ 4.62-4.63 (d, 2H, *J* = 5.77 Hz), δ 5.22-5.24 (d, 1H, *J* = 10.41 Hz), δ 5.29-5.34 (dd, 1H, *J* = 1.31, 17.19 Hz), δ 5.86-5.93 (m, 1H), δ 6.85 (s, 1H), δ 7.28-7.33 (m, 2H), δ 7.97-8.00 (d, 1H, *J* = 8.89 Hz). ^{13}C NMR (100 MHz, $CDCl_3$): δ 21.43, 66.43, 115.78, 118.91, 121.07, 126.79, 131.84, 136.26, 142.29, 143.88, 152.57. LCMS-ESI (Method E) (m/z): $C_{11}H_{12}N_2O_4$ (236.22) [M-H$^+$] found 235.0; retention time 7.75 min.

Allyl (4-amino-3-methylphenyl) carbamate (**18b, JP-193-14**) **17b** (0.080 g, 0.339 mmol, 1 eq) was dissolved in 2 mL EtOH/H_2O solvent mixture (ratio: 3/1), added with iron powder (0.114 g, 2.034 mmol, 6 eq) and NH_4Cl (0.163 g, 3.051 mmol, 9 eq). The suspension was stirred at 80°C for 2h. Once the reaction was confirmed finished via TLC, the reaction was quenched by cooling

View Article Online
DOI: 10.1039/D5MD00316D

the reaction to r.t., and the suspension was filtered via Celite. The filtered organic layer was evaporated in a rotary evaporator and redissolved in EA, washed with water, brine, and dried over $MgSO_4$. The solvent was then filtered and evaporated in a rotary evaporator, fully dried to obtain 0.096 g product and it was directly used without further purification. ^{1}H NMR (400 MHz, DMSO-d4): δ 2.01 (s, 3H), δ 4.53-4.55 (m, 4H), δ 5.19-5.22 (d, 1H, J = 10.40 Hz), δ 5.30-5,35 (d, 1H, J = 17.19 Hz), δ 5.91-6.00 (m, 1H), δ 6.50-6.52 (d, 1H, J = 8.38 Hz), δ 6.94-6.99 (m, 2H), δ 9.12 (s, 1H). LCMS-ESI (m/z): $[M+H]^+$ calcd for $C_{11}H_{14}N_2O_2$ 207.25; found 207.1; retention time 4.03 min (Method E).

Allyl 8-(4-((4-(((allyloxy) carbonyl) amino)-2-methylphenyl) amino)-4-oxobutoxy)-7-methoxy-5-oxo-11-((tetrahydro-2H-pyran-2-yl)oxy)-2,3,11,11a-tetrahydro-1H-benzo[e]pyrrolo[1,2-a][1,4]diazepine-10(5H)-carboxylate (**19b, JP-193-15**) **8** (0.090 g, 0.174 mmol, 1 eq) was dissolved in 3 mL DMF, added with DMAP (0.083 g, 0.348 mmol, 2 eq) and EDC (0.083 g, 0.248 mmol, 2.5 eq). The mixture was stirred for 30 mins, then added **18b** to leave the reaction stirred at r.t. overnight. The reaction was quenched with 10× volume H_2O, and it was extracted with 3 × 30 mL EA, the organic layer was combined with and washed with 100 mL 1M citric acid, 100 mL water, 100 mL brine, and dried over $MgSO_4$. The organic layer was evaporated in a rotary evaporator and purified using flash column chromatography (0-70% EA in Hexane). *Rf*=0.26 (TLC: Hex/EA = 3/7). The product was collected and evaporated in a rotary evaporator, followed by high vac drying, yielding 0.119 g (Yield: 96.0%). ^{1}H NMR (400 MHz, MeOD-d4): δ 1.41-1.63 (m, 4H), δ 1.63-1.89 (m, 2H), δ 2.0-2.10 (m, 3H), δ 2.10-2.89 (m, 6H), δ 2.56-2.71 (m, 2H), δ 3.43-3.54 (m, 2H), δ 3.54-3.69 (m, 2H), δ 3.84-4.01 (m, 4H), δ 4.09-4.18 (m, 3H), δ 4.30-4.74 (m, 4H), δ 5.02-5.14 (m, 2H), δ 5.21-5.24 (d, 1H, J = 10.47 Hz), δ 5.33-5.38 (dd, 1H, J = 17.23, 1.36 Hz), δ 5.77-5.80 (m, 1H), δ 5.88-5.90 (d, 1H, J = 9.40 Hz), δ 5.94-6.04 (m, 1H), δ 6.96-6.98 (d, 1H, J = 7.96 Hz), δ 7.19-7.21 (m, 2H), δ 7.25-7.27 (d, 1H, J = 8.69 Hz), δ 7.31 (s, 1H). LCMS-ESI (Method E) (m/z): $C_{37}H_{46}N_4O_{10}$ (706.79) $[M+Na^+]$ 729.3; retention time 7.68 min.

(S)-N-(4-amino-2-methylphenyl)-4-((7-methoxy-5-oxo-2,3,5,11a-tetrahydro-1H-benzo[e]pyrrolo[1,2-a][1,4]diazepin-8-yl)oxy)butanamide (**20b, JP-193-16**) **19b** (0.111 g, 0.157 mmol, 1 eq) was dissolved 5 mL DCM, added with PPh_3 (0.021 g, 0.079 mmol, 0.5 eq), palladium tetrakis[triphenylphosphine] (0.019 g, 0.016 mmol, 0.1 eq), and pyrrolidine (0.020 mL, 0.236 mmol, 1.5 eq). The solvent was stirred for 2h. The reaction was quenched via evaporation in a rotary evaporator and dried in high vac. The crude was further purified using column chromatography (0-10% MeOH in EA). *Rf*=0.36 (TLC: EA/MeOH = 8/2) The product was collected, evaporated in a rotary evaporator, and dried in high vac. 0.047 g of product was obtained (Yield: 68.3%). ^{1}H NMR (400 MHz, DMSO-d6): δ 1.88-1.95 (m, 2H), δ 2.01-2.05 (m, 5H), δ 2.18-2.27 (m, 2H), δ 2.41-2.45 (t, 2H, *J* = 7.05 Hz), δ 3.39-3.51 (m,2H), δ 3.57-3.62 (m, 1H), δ 3.67 (s, 3H), δ 3.93-3.98 (m, 2H), δ 4.88 (s, 2H), δ 6.08-6.17 (m, 1H), δ 6.37-6.39 (m, 1H), δ 6.84-6.87 (m, 1H), δ 7.06-7.10 (m, 1H), δ 7.26-7.35 (m, 1H), δ 7.78-7.79 (d, 1H, *J* = 4.42 Hz), δ 9.02 (m, 1H). ^{13}C NMR (100 MHz, DMSO-d6): δ 18.46, 22.88-23.05, 24.14, 25.34-25.47, 32.40, 53.88-54.21, 56.09-56.34, 58.58-58.86, 67.85-68.35, 101.98, 110.05-110.63, 111.73-111.86, 115.39-115.67, 125.57, 127.26-127.46, 133.93, 138.77-139.74, 141.06-141.16, 146.92-147.42, 150.70, 152.05, 163.83, 164.72-165.28, 170.91. LCMS-ESI (Method E) (m/z): $C_{24}H_{29}N_4O_4$ (436.51) $[M+H^+]$ 437.2; product peak retention time at 4.13 min, purity: 98.5%. LCMS-ESI (Method F) (m/z): product peak retention time at 1.94 min, purity > 98.5%. HRMS-ESI: $C_{24}H_{28}N_4O_4$ (436.51) $[M+H^+]$ calculated 437.21833; found 437.2179; error -1.03 ppm.

Allyl (3-methoxy-4-nitrophenyl) carbamate (**17c, JP-193-18**) 3-Methoxy-4-nitroaniline (**16c**, 0.100 g, 0.595 mmol, 1 eq) was dissolved in 2 mL DMF, which was added with K_2CO_3 (0.099 g, 0.714 mmol, 1.2 eq) and 97% allyl chloroformate (0.07 mL, 0.655 mmol, 1.1 eq). The mixture was allowed to stir at r.t. overnight. After the reaction was finished (confirmed by TLC), it was quenched by 10 mL DCM, and it was washed with 10 sat. $CuSO_4$, 3 × 10 mL water, 3 × 10 mL Na_2CO_3. The organic layer was then dried over sodium sulphate, filtered, and then evaporated via rotary evaporator. The crude was purified using flash column chromatography (0-20% EA in hexane). *Rf*=0.60 (TLC: Hexane/EA = 6/4). The product was collected and evaporated in a rotary evaporator, gaining 0.129 g product after fully dried in high vac (Yield: 85.6%). ^{1}H NMR (400 MHz, $CDCl_3$): δ 2.97 (s, 3H), δ 4.68-4.70 (d, 2H, *J* = 5.76 Hz), δ 5.28-5.40 (m, 2H), δ 5.91-6.00 (m, 1H), δ 6.73-6.75 (dd, 1H, *J* = 2.08, 8.92 Hz), δ 6.95 (s, 1H), δ 7.58 (d, 1H, *J* = 1.21 Hz), δ 7.92-7.95 (d, 1H, *J* = 8.91 Hz), ^{13}C NMR (100 MHz, $CDCl_3$): δ 56.56, 66.46, 102.42, 109.12, 118.97, 127.62, 131.74, 134.14, 143.97, 152.56, 155.17. LCMS-ESI (Method E) (m/z): $C_{11}H_{12}N_2O_5$ (252.23) $[M-H^+]$ found 251.1; retention time 7.37 min.

Allyl (4-amino-3-methoxyphenyl) carbamate (**18c, JP-163-19**) **17c** (0.090 g, 0.358 mmol, 1 eq) was dissolved in 2 mL EtOH/H_2O solvent mixture (ratio: 3/1), added with iron powder (0.120 g, 2.148 mmol, 6 eq) and NH_4Cl (0.172 g, 3.222 mmol, 9 eq). The suspension was stirred at 80°C for 2h. Once the reaction was confirmed finished using TLC, the reaction was quenched by cooling to r.t., and the suspension was filtered via Celite. The filtered organic layer was evaporated in a rotary evaporator and redissolved in EA, washed with water, brine, and dried over $MgSO_4$. The solvent was then filtered and evaporated in a rotary evaporator, fully dried to obtain 0.066 g product, which was directly used without further purification. ^{1}H NMR (400 MHz, DMSO-d6): δ 3.71 (s, 3H), δ 4.42 (s, 2H), δ 4.55-4.56 (d, 2H, *J* = 5.39 Hz), δ 5.20-5.23 (dd, 1H, *J* = 10.46,1.32 Hz), δ 5.31-5.36 (dd, 1H, *J* = 17.22, 1.42 Hz), δ 5.91-6.01 (m, 1H), δ 6.52-6,54 (d, 1H, *J* = 8.32 Hz), δ 6.71-6.73 (d, 1H, *J* = 7.85 Hz), δ 7.01 (s, 1H), δ 9.23 (s, 1H). ^{13}C NMR (100 MHz, DMSO-d6): δ 55.63, 64.74, 103.59, 112.01, 114.08, 117.70, 129.21, 133.53, 134.08, 146.66, 153.85, 212.05. LCMS-ESI (Method E) (m/z): $C_{11}H_{14}N_2O_3$ (222.24) $[M+H^+]$ 223.1; retention time 4.01 min.

Allyl 8-(4-((4-(((allyloxy) carbonyl) amino)-2-methoxyphenyl) amino)-4-oxobutoxy)-7-methoxy-5-oxo-11-((tetrahydro-2H-pyran-2-yl)oxy)-2,3,11,11a-tetrahydro-1H-benzo[e]pyrrolo[1,2-a][1,4]diazepine-10(5H)-carboxylate (**19c, JP-193-20**) **8** (0.090 g, 0.174 mmol, 1 eq) was dissolved in 3 mL DMF, added with DMAP (0.043 g, 0.348 mmol, 2 eq) and EDC (0.083 g, 0.435 mmol, 2.5 eq). The mixture was stirred for 30 mins, then added **18c** to leave the reaction stirred at r.t. overnight. The reaction was quenched with 10× volume H_2O, and it was extracted with 3 × 30 mL EA, the organic layer was combined with and washed with 100 mL 1M citric acid, 100 mL water, 100 mL brine, and dried over $MgSO_4$. The organic layer was evaporated in a rotary evaporator and purified using flash column chromatography (0-100% EA in Hexane). *Rf*=0.22 (TLC: Hex/EA = 4/6). The product was collected and

View Article Online
DOI: 10.1039/D5MD00316D

evaporated in a rotary evaporator, followed by drying in high vac, which obtained 0.135 g (Yield > 99.9%). ^{1}H NMR (400 MHz, MeOD-d4): δ 1.45-1.60 (m, 4H), δ 1.70-1.79 (m, 2H), δ 2.01-2.08 (m, 2H), δ 2.09-2.23 (m, 4H), δ 2.54-2.69 (m, 2H), δ 3.42-3.53 (m, 2H), δ 3.53-3.69 (m, 2H), δ 3.79-3.80 (d, 3H, *J* = 3.42 Hz), δ 3.87 (s, 3H), δ 3.89-3.98 (m, 1H), δ 4.07-4.13 (q, 3H, *J* = 7.11 Hz), δ 4.39-4.64 (m, 4H), δ 5.05-5.08 (d, 2H, *J* = 14.47 Hz), δ 5.21-5.24 (d, 1H, *J* = 10.52 Hz), δ 5.34-5.38 (d, 1H, *J* = 17.26 Hz), δ 5.76-5.79 (d, 1H, *J* = 9.64 Hz), δ 5.87-5.89 (d, 1H, *J* = 9.32 Hz), δ 5.95-6.04 (m, 1H), δ 6.86-6.89 (m, 2H), δ 6.96 (s, 1H), δ 7.18-7.20 (d, 1H, *J* = 7.76 Hz), δ 7.29 (s, 1H), δ 7.78-7.80 (d, 1H, *J* = 8.68 Hz). LCMS-ESI (Method E) (m/z): $C_{37}H_{46}N_4O_{11}$ (722.8) [M+Na$^+$] 745.3; retention time 7.80 min.

(S)-N-(4-amino-2-methoxyphenyl)-4-((7-methoxy-5-oxo-2,3,5,11a-tetrahydro-1H-benzo[e]pyrrolo[1,2-a][1,4]diazepin-8-yl)oxy)butanamide (**20c, JP-193-21**) **19c** (0.124 g, 0.172 mmol, 1 eq) was dissolved 5 mL DCM, added with PPh_3 (0.023 g, 0.086 mmol, 0.5 eq), palladium tetrakis[triphenylphosphine] (0.020 g, 0.017 mmol, 0.1 eq), and pyrrolidine (0.022 mL, 0.258 mmol, 1.5 eq). The solvent was stirred for 2h. The reaction was quenched via evaporation in a rotary evaporator and dried in high vac. The crude was further purified using flash column chromatography (0-10% MeOH in EA). *Rf*=0.42 (TLC: EA/MeOH = 8/2) The product was collected, evaporated in a rotary evaporator, and dried in high vac. 0.050 g product was obtained (Yield: 64.8%). ^{1}H NMR (400 MHz, DMSO-d6): δ 1.76-1.90 (m, 2H), δ 1.98-2.03 (m, 2H), δ 2.18-2.31 (m, 2H), δ 2.43-2.46 (t, 2H, *J* = 7.36 Hz), δ 3.39-3.42 (m, 2H), δ 3.57-3.63 (m, 1H) δ 3.68 (s, 3H), δ 3.83 (s, 3H), δ 3.91 (s 2H), δ 4.10-4.13 (m, 2H), δ 6.08-6.11 (dd, 1H, J = 8.27, 2.18 Hz), δ 6.23-6.26 (m, 1H), δ 6.84 (s, 1H), δ 7.24-7.26 (d, 1H, *J* = 8.31 Hz), δ 7.34 (s, 1H), δ 7.78-7.79 (d, 1H, *J* = 4.40 Hz), δ 8.88 (m, 1H). ^{13}C NMR (100 MHz, DMSO-d6): δ 22.56, 24.14, 25.27, 29.16-29.46, 31.75, 32.57, 49.07, 55.55-55.73, 56.09-56.30, 68.29, 98.19, 105.64, 110.61, 111.74, 116.35, 120.25, 125.74, 141.07, 147.41, 150.70, 163.83, 164.72, 170.63. LCMS-ESI (Method E) (m/z): $C_{24}H_{29}N_4O_5$ (452.21) [M+H$^+$] 453.2; retention time 4.21 min; purity: 92.5%. LCMS-ESI (Method F) (m/z): retention time at 1.98 min, purity > 98.5%. HRMS-ESI: $C_{24}H_{29}N_4O_5$ (452.21) [M+H$^+$] calculated 453.21325; found 453.2129; error -0.69 ppm.

Cell culture. CLL cells, the CLL cell line, MEC-1, the breast cancer cell line, MDA-MB-231 and the lenalidomide resistant myeloma cell line, RPMI-8226 were selected for testing cytotoxicity of the PROTAC molecules. Primary CLL cells were collected from patients and normal B- and T-lymphocytes were obtained from healthy volunteers. All experiments were performed in accordance with the U.K. Human Tissue Authority guidelines, and experiments were approved by the local research ethics committee (17/SW/0263). Informed consent was obtained from all human participants in this study. Cell lines were acquired from DSMZ (MEC-1 and RPMI-8226) or ATCC (MDA-MB-231); cells were maintained in RPMI 1640 media (primary CLL cells, MEC-1 and RPMI-8226) or DMEM media (MDA-MB-231) with the addition of 10% FBS, 1% L-Glutamine, and 1% penicillin streptomycin. The cells were seeded 500,000 cells/mL at 37°C in a humidified atmosphere containing 5% CO_2. The cells were split every 48 hours; cell count and viability were measured each time.

Cell counting. 10µL of cell suspension was mixed with 10µL of trypan blue. Subsequently, 10µL of the mixture was pipetted into a cell counting slide. The slide was inserted into a Countess 3 cell counter (ThermoFisher scientific) to quantify the cell count and cell viability.

Apoptotic assay for RelA/p65-targeting PROTACs. 500,000 cells/well were aliquoted into 24-well plates following resuspension with 1 mL of appropriate medium. All test compounds were dissolved in DMSO as 1mM stock solution. Subsequently, working stocks of the PROTACs, and their individual constituent molecules, were produced by serial dilutions in a 96-well plate: RelA/p65-targeting PROTACs (1µM, 0.5µM and 0.25µM, 0.125µM, and 0.0625µM). 10 µL of each dilution was then transferred to the cell suspensions in the 24-well plate. The plates were then incubated for 48 hours at 37°C with 5% CO_2. Samples were then harvested into 1.5 mL Eppendorf tubes and centrifuged at 500x*g* for 5 mins. The supernatant was then poured off and the cell pellets resuspended in 96 µL Annexin V binding buffer and 4µL FITC Annexin V (both Biolegend) was added to each tube. The tubes were then incubated in dark for 10 mins prior to the addition of 4µL 7-AAD. Finally, the cells were analysed using a CytoFLEX LX (Beckman Coulter) flow cytometer. In all cases, 10,000 events were recorded. Apoptosis was quantified using CytExpert software, while the percentage of apoptotic cells was defined as Annexin-V positive and 7-AAD positive, or Annexin-V positive and 7-AAD negative. The data was further analysed using GraphPad prism to calculate the LC_{50} values for each compound using non-linear regression analysis.

Evaluation of NF-κB subunit expression following treatment with PROTAC. Aliquots of 0.5 x 10^6 MEC-1 cells were treated with increasing concentrations of **15d** for 24 h. Cells were harvested by centrifugation, fixed using Cyto-Fast™ fix/perm buffer set (Biolegend) buffer for 20 mins at 37°C. Cells were then washed in Cyto-Fast™ Perm Wash solution and centrifuged at 300x*g* for 5 mins before being resuspended in 100 µL Perm Wash solution followed by the addition of 5µL APC-labelled RelA/p65 antibody (Biolegend), 5µL PE-labelled cRel antibody (eBiosciences) and 5µL corallite 488-labelled RelB antibody (ThermoFisher). Cells were incubated for 20 mins prior to washing in cell staining buffer, centrifugation at 300x*g* for 5 mins and resuspension in 100µL cell staining buffer prior to acquisition of the data on a CytoFLEX LX flow cytometer.

MG-132 proteasome inhibition assay. To determine whether the toxicity of **15d** was dependent on proteasome activity, MDA-MB-231 cells were treated with increasing concentrations of the proteasome inhibitor, MG-132 (0.1µM – 10µM) for 48 h. Aliquots of cells were first assessed for their apoptotic response to MG-132 using Annexin V and 7-AAD labelling (as described above). In parallel, proteasome activity was assessed using a proteasome activity assay kit (Abcam). The kit uses an AMC-tagged peptide substrate (Proteasome Substrate (Succ-LLVY-AMC in DMSO), which releases free, highly fluorescent AMC (Ex/Em 350/440 nm) in the presence of proteolytic activity. MEC-1 cells were very sensitive to the cytotoxic effects of MG-132. So, in this cell line, combination studies were carried out with 0.18µM MG-132. Treatment of MEC-1 cells with 0.18µM MG-132 caused >40% reduction in proteasome activity without significant effects on cellular viability. Subsequently, 10µL MG-132 stock was added to the 500,000 cells/mL MEC-1 cell with increasing concentrations of **15d** or the PBD building block, **20d**. All treated cells were cultured for 48 h at 37°C with 5% CO_2. The cells were then harvested by

View Article Online
DOI: 10.1039/D5MD00316D

centrifugation (300x*g* for 5 mins) and then incubated with annexin V and 7-AAD, prior to analysis by flow cytometry (as described above.).

FRET melting Assay The single-strand oligonucleotide FRET hairpin was purchased from Eurogentec Ltd, tagged with TAM at 5' and TAMRA at 3' terminal (sequence: 5'-FAM- TAT-AAG-ATA-TAT-ATA-TTT-TTT-TAT-ATA-TAT-CTT-ATA-TAMRA-3'). Nuclease-free water was added to prepare 20µM ssDNA stock solution, and it was further diluted to 400 nM using 50mM K Cacodylate buffer (pH = 7.4). The prepared ssDNA sample was annealed at 85°C for 5 mins and then allowed to cool down to room temperature and then store in -20°C for completing annealing process. PBD controls and PROTACs were prepared as 20µM working solution diluted by 50mM K Cacodylate buffer (pH = 7.4). 25µL compound working solution was added to 25 µl DNA stock in the well of the Bio-Rad 96-well plate. DNA Engine Opticom was used for melting. The sample was initially incubated at 30°C for 3 h and then gradually increasing the temperature to 100°C. The fluorescence signal was detected at intervals of 0.5°C. The mean of the melting point was analysed via GraphPad prism, and the melting point difference between the sample and naked ssDNA (ΔTm) was calculated for comparison.

Data analysis All biological data was calculated and plotted in GraphPad Prism. The standard deviations were presented as error bars in the plotted graph. The sigmoid dose-response curves were plotted using non-linear regression (4 parameters) to obtaining LC_{50} values (the concentration of drug required to kill 50% of the cells in culture). As for significance testing, the mean values in the two groups were measured and compared. The data were initially subjected to normality testing using the Shapiro-Wilk and Kolmogorov-Smirnov test. If the data passed the normality test, it was then further evaluated using a paired t-test to assess whether there was a significance in the data before and after treatment. It was considered significantly different when p value of the testing groups <0.05 with 95% confidence interval. If the data failed the normality test, they were subsequently evaluated using the Kruskal-Wallis test with Dunn's multiple comparison *post hoc* correction, if more than one set of pairs were analysed.

ASSOCIATED CONTENT

Supporting Information

The Supporting Information is available on the Publications website.

^{1}H NMR, ^{13}C NMR, LC-MS spectrum of the final products. 2D docking results of short benzene-fused PBDs. (docx)

HRMS spectrum of the final products (PDF)

AUTHOR INFORMATION

Corresponding Authors

Chris Pepper Brighton and Sussex Medical School, University of Brighton and University of Sussex, Brighton BN1 9PX, U.K.

c.pepper@bsms.ac.uk orcid ID: 0000-0003-3603-8839

Khondaker Miraz Rahman Institute of Pharmaceutical Science, School of Cancer and Pharmaceutical Sciences, King's College London, London SE1 9NH, U.K.

k.miraz.rahman@kcl.ac.uk orcid ID: 0000-0001-8566-8648

Authors

Peiqin Jin Institute of Pharmaceutical Science, School of Cancer and Pharmaceutical Sciences, King's College London, London SE1 9NH, U.K.

Md. Mahbub Hasan Institute of Pharmaceutical Science, School of Cancer and Pharmaceutical Sciences, King's College London, London SE1 9NH, U.K. Current address: Department of Genetic Engineering and Biotechnology, Faculty of Biological Sciences, University of Chittagong, Chattogram, 4331, Bangladesh.

Andrea G.S. Pepper Brighton and Sussex Medical School, University of Brighton and University of Sussex, Brighton BN1 9PX, U.K.

Simon Mitchell Brighton and Sussex Medical School, University of Brighton and University of Sussex, Brighton BN1 9PX, U.K.

Author Contributions

K.M.R. and C.P. contributed equally. J.P., M.M.H., A.G.S.P, S.M., K.M.R., and C.P. designed the experiments and analysed the data. J.P., and M.M.H. designed, synthesized, and analysed the compounds. J.P., A.G.S.P., and C.P. performed the biological experiments. J.P., M.M.H., and K.M.R. performed the docking studies. J.P., K.M.R., and C.P. wrote the manuscript, with edits from M.M.H., A.G.S.P., and S.M.

Funding Sources

This research was funded in part by a self-funded PhD studentship (P.J.) and by personal research funding held by C.P.

Conflicts of Interest

The authors have no relevant conflicts of interest**.**

Data Availability

The data supporting this article have been included as part of the Supplementary Information.

ACKNOWLEDGMENTS

The chemistry work was performed at King's College London, while the biology evaluations were performed at Brighton and Sussex Medical School, University of Sussex. **20d** (MMH-165-26) and **3** (MMH-165-31) were obtained from Md. Mahbub Hassan.

ABBREVIATIONS

7-AAD, 7-Aminoactinomycin D; BAIB, Bis(acetoxy)iodobenzene; CRBN, Cereblon; DCM, Dichloromethane; dd, double of doublets; DHP, Dihydropyran; DMAP, 4-dimethylaminopyridine; DMF, Dimethylformamide; DMSO, Dimethyl sulfoxide; EA, Ethyl acetate; EDC, 1-Ethyl-3-(3-dimethyl aminopropyl) carbodiimide; FBS, Fetal bovine serum; FITC, Fluorescein isothiocyanate; FRET, Fluorescence resonance energy transfer; G, Guanine; HPLC, High performance liquid chromatography; HRMS, High Resolution Mass Spectrometry; ImiDs, Immunomodulatory drugs; LC_{50}, Concentration of the toxic substance lethal to half of test cells; LC-

View Article Online
DOI: 10.1039/D5MD00316D

MS, Liquid chromatography–mass spectrometry; Lys, Lysine; m, multiplet; M, Molar; NF-κB, Nuclear transcription *kappa* B; nM, nanomolar; NMP, N-Methyl-2-pyrrolidone; NMR, Nuclear magnetic resonance; PBD, Pyrrolobenzodiazepine; PBS, Phosphate-buffered saline; PROTAC, Proteolysis targeting chimera; q, quartet; RPMI, Roswell Park Memorial Institute; s, singlet; SAR, Structure-activity relationships; ssDNA, single-stranded DNA; T, Thymine; t, triplet; TAMRA, Carboxytetramethylrhodamine; TEMPO, (2,2,6,6-Tetramethylpiperidin-1-yl)oxyl; TF, Transcription factor; TFA, Trifluoroacetic acid; THF, Tetrahydrofuran; TLC, Thin-layer chromatography; TPD, Targeted protein degradation; UV, Ultraviolet; ΔTm, Variation of the melting temperature; *m/z*, mass-to-charge ratio.

REFERENCES

1. Liu, T.; Zhang, L.; Joo, D.; Sun, S.-C. NF-KB Signaling in Inflammation. *Signal Transduct Target Ther* **2017**, *2* (1), 17023.

2. Taniguchi, K.; Karin, M. NF-KB, Inflammation, Immunity and Cancer: Coming of Age. *Nat Rev Immunol* **2018**, *18* (5), 309–324.

3. Duran, C. L.; Karagiannis, G. S.; Chen, X.; Sharma, V. P.; Entenberg, D.; Condeelis, J. S.; Oktay, M. H. Cooperative NF-KB and Notch1 Signaling Promotes Macrophage-Mediated MenaINV Expression in Breast Cancer. *Breast Cancer Research* **2023**, *25* (1), 37.

4. Hewamana, S.; Alghazal, S.; Lin, T. T.; Clement, M.; Jenkins, C.; Guzman, M. L.; Jordan, C. T.; Neelakantan, S.; Crooks, P. A.; Burnett, A. K.; Pratt, G.; Fegan, C.; Rowntree, C.; Brennan, P.; Pepper, C. The NF-KB Subunit Rel A Is Associated with in Vitro Survival and Clinical Disease Progression in Chronic Lymphocytic Leukemia and Represents a Promising Therapeutic Target. *Blood* **2008**, *111* (9), 4681–4689.

5. Verzella, D.; Pescatore, A.; Capece, D.; Vecchiotti, D.; Ursini, M. V.; Franzoso, G.; Alesse, E.; Zazzeroni, F. Life, Death, and Autophagy in Cancer: NF-KB Turns up Everywhere. *Cell Death Dis* **2020**, *11* (3), 210.

6. Bhagwat, A. S.; Vakoc, C. R. Targeting Transcription Factors in Cancer. *Trends Cancer* **2015**, *1* (1), 53–65.

7. Li, K.; Crews, C. M. PROTACs: Past, Present and Future. *Chem Soc Rev* **2022**, *51* (12), 5214–5236.

8. Zhuang, J.; Liu, Q.; Wu, D.; Tie, L. Current Strategies and Progress for Targeting the "Undruggable" Transcription Factors. *Acta Pharmacol Sin* **2022**, *43* (10), 2474–2481.

9. Horie, K.; Ma, J.; Umezawa, K. Inhibition of Canonical NF-KB Nuclear Localization by (−)-DHMEQ via Impairment of DNA Binding. *Oncology Research Featuring Preclinical and Clinical Cancer Therapeutics* **2015**, *22* (2), 105–115.

10. Shono, Y.; Tuckett, A. Z.; Ouk, S.; Liou, H.-C.; Altan-Bonnet, G.; Tsai, J. J.; Oyler, J. E.; Smith, O. M.; West, M. L.; Singer, N. V.; Doubrovina, E.; Pankov, D.; Undhad, C. V.; Murphy, G. F.; Lezcano, C.; Liu, C.; O'Reilly, R. J.; van den Brink, M. R. M.; Zakrzewski, J. L. A Small-Molecule c-Rel Inhibitor Reduces Alloactivation of T Cells without Compromising Antitumor Activity. *Cancer Discov* **2014**, *4* (5), 578–591.

11. Thurston, D. E.; Pysz, I. *Chemistry and Pharmacology of Anticancer Drugs*; CRC Press: Second edition. | Boca Raton: CRC Press, 2021.

12. Corcoran, D. B.; Lewis, T.; Nahar, K. S.; Jamshidi, S.; Fegan, C.; Pepper, C.; Thurston, D. E.; Rahman, K. Miraz. Effects of Systematic Shortening of Noncovalent C8 Side Chain on the Cytotoxicity and NF-KB Inhibitory Capacity of Pyrrolobenzodiazepines (PBDs). *J Med Chem* **2019**, *62* (4), 2127–2139.

13. Hu, W.-P.; Tsai, F.-Y.; Yu, H.-S.; Sung, P.-J.; Chang, L.-S.; Wang, J.-J. Induction of Apoptosis by DC-81-Indole Conjugate Agent Through NF-KB and JNK/AP-1 Pathway. *Chem Res Toxicol* **2008**, *21* (7), 1330–1336.

14. Rahman, K. M.; Jackson, P. J. M.; James, C. H.; Basu, B. P.; Hartley, J. A.; de la Fuente, M.; Schatzlein, A.; Robson, M.; Pedley, R. B.; Pepper, C.; Fox, K. R.; Howard, P. W.; Thurston, D. E. GC-Targeted C8-Linked Pyrrolobenzodiazepine–Biaryl Conjugates with Femtomolar in Vitro Cytotoxicity and in Vivo Antitumor Activity in Mouse Models. *J Med Chem* **2013**, *56* (7), 2911–2935.

15. Kanzaki, H.; Chatterjee, A.; Hossein, H.; Zhang, X.; Chung, S.; Deng, N.; Ramanujan, V. K.; Cui, X.; Greene, M. I.; Murali, R. Disabling the Nuclear Translocalization of RelA/NF-KB by a Small Molecule Inhibits Triple-Negative Breast Cancer Growth. *Breast Cancer: Targets and Therapy* **2021**, *Volume 13*, 419–430.

16. Zou, Y.; Ma, D.; Wang, Y. The PROTAC Technology in Drug Development. *Cell Biochem Funct* **2019**, *37* (1), 21–30.

17. Paiva, S.-L.; Crews, C. M. Targeted Protein Degradation: Elements of PROTAC Design. *Curr Opin Chem Biol* **2019**, *50*, 111–119.

18. Pettersson, M.; Crews, C. M. PROteolysis TArgeting Chimeras (PROTACs) — Past, Present and Future. *Drug Discov Today Technol* **2019**, *31*, 15–27.

19. Bondeson, D. P.; Smith, B. E.; Burslem, G. M.; Buhimschi, A. D.; Hines, J.; Jaime-Figueroa, S.; Wang, J.; Hamman, B. D.; Ishchenko, A.; Crews, C. M. Lessons in PROTAC Design from Selective Degradation with a Promiscuous Warhead. *Cell Chem Biol* **2018**, *25* (1), 78-87.

20. Guenette, R. G.; Yang, S. W.; Min, J.; Pei, B.; Potts, P. R. Target and Tissue Selectivity of PROTAC Degraders. *Chem Soc Rev* **2022**, *51* (14), 5740–5756.

View Article Online
DOI: 10.1039/D5MD00316D

21. Mannion, J.; Gifford, V.; Bellenie, B.; Fernando, W.; Ramos Garcia, L.; Wilson, R.; John, S. W.; Udainiya, S.; Patin, E. C.; Tiu, C.; Smith, A.; Goicoechea, M.; Craxton, A.; Moraes de Vasconcelos, N.; Guppy, N.; Cheung, K. M. J.; Cundy, N. J.; Pierrat, O.; Brennan, A.; Roumeliotis, T. I.; Benstead-Hume, G.; Alexander, J.; Muirhead, G.; Layzell, S.; Lyu, W.; Roulstone, V.; Allen, M.; Baldock, H.; Legrand, A.; Gabel, F.; Serrano-Aparicio, N.; Starling, C.; Guo, H.; Upton, J.; Gyrd-Hansen, M.; MacFarlane, M.; Seddon, B.; Raynaud, F.; Roxanis, I.; Harrington, K.; Haider, S.; Choudhary, J. S.; Hoelder, S.; Tenev, T.; Meier, P. A RIPK1-Specific PROTAC Degrader Achieves Potent Antitumor Activity by Enhancing Immunogenic Cell Death. *Immunity* **2024**, *57* (7), 1514-1532.

22. Liu, J.; Chen, H.; Kaniskan, H. Ü.; Xie, L.; Chen, X.; Jin, J.; Wei, W. TF-PROTACs Enable Targeted Degradation of Transcription Factors. *J Am Chem Soc* **2021**, *143* (23), 8902–8910.

23. Surani, Y.; Wand, M.; Picconi, P.; Di Palma, M.; Zenezini Chiozzi, R.; Hasan, M.; & Maynard-Smith, M.; Steiner, R.; Rahman, K.; Hind, C.; Sutton, Mark. Convergent evolution of antibiotic resistance mechanisms between synthetic pyrrolobenzodiazepines (PBDs) and the naturally occurring albicidin in multidrug resistant Klebsiella pneumoniae. 10.21203/rs.3.rs-4901630/v1.

24. Zhou, H.; Bai, L.; Xu, R.; McEachern, D.; Chinnaswamy, K.; Li, R.; Wen, B.; Wang, M.; Yang, C.-Y.; Meagher, J. L.; Sun, D.; Stuckey, J. A.; Wang, S. SD-91 as A Potent and Selective STAT3 Degrader Capable of Achieving Complete and Long-Lasting Tumor Regression. *ACS Med Chem Lett* **2021**, *12* (6), 996–1004.

25. Patel, U.; Smalley, J. P.; Hodgkinson, J. T. PROTAC Chemcal Probes for Histone Deacetylase Enzymes. *RSC Chem Biol* **2023**, *4* (9), 623–634.

26. Qiu, X.; Sun, N.; Kong, Y.; Li, Y.; Yang, X.; Jiang, B. Chemoselective Synthesis of Lenalidomide-Based PROTAC Library Using Alkylation Reaction. *Org Lett* **2019**, *21* (10), 3838–3841.

27. Pettersson, M.; Crews, C. M. PROteolysis TArgeting Chimeras (PROTACs) — Past, Present and Future. *Drug Discov Today Technol* **2019**, *31*, 15–27.

28. Riching, K. M.; Caine, E. A.; Urh, M.; Daniels, D. L. The Importance of Cellular Degradation Kinetics for Understanding Mechanisms in Targeted Protein Degradation. *Chem Soc Rev* **2022**, *51* (14), 6210–6221.

29. Heider M, Eichner R, Stroh J, Morath V, Kuisl A, Zecha J, Lawatscheck J, Baek K, Garz AK, Rudelius M, Deuschle FC, Keller U, Lemeer S, Verbeek M, Götze KS, Skerra A, Weber WA, Buchner J, Schulman BA, Kuster B, Fernández-Sáiz V, Bassermann F. The IMiD target CRBN determines HSP90 activity toward transmembrane proteins essential in multiple myeloma. Mol Cell. 2021 Mar 18;81(6):1170-1186.e10. doi: 10.1016/j.molcel.2020.12.046. Epub 2021 Feb 10. PMID: 33571422; PMCID: PMC7980223.

30. Kassam, F.; Enright, K.; Dent, R.; Dranitsaris, G.; Myers, J.; Flynn, C.; Fralick, M.; Kumar, R.; Clemons, M. Survival Outcomes for Patients with Metastatic Triple-Negative Breast Cancer: Implications for Clinical Practice and Trial Design. *Clin Breast Cancer* **2009**, *9* (1), 29–33.

31. Espinoza-Sánchez, N. A.; Enciso, J.; Pelayo, R.; Fuentes-Pananá, E. M. *An NFκB-Dependent Mechanism of Tumor Cell Plasticity and Lateral Transmission of Aggressive Features*; 2018; Vol. 9.

32. Winzker, M.; Friese, A.; Koch, U.; Janning, P.; Ziegler, S.; Waldmann, H. Development of a PDEδ-Targeting PROTACs That Impair Lipid Metabolism. *Angewandte Chemie* **2020**, *132* (14), 5644–5650.

33. Zhang, Y.; Yang, B.; Zhao, J.; Li, X.; Zhang, L.; Zhai, Z. Proteasome Inhibitor Carbobenzoxy-L-Leucyl-L-Leucyl-L-Leucinal (MG132) Enhances Therapeutic Effect of Paclitaxel on Breast Cancer by Inhibiting Nuclear Factor (NF)-KB Signaling. *Medical Science Monitor* **2018**, *24*, 294–304.

34. Ferguson, L.; Bhakta, S.; Fox, K. R.; Wells, G.; Brucoli, F. Synthesis and Biological Evaluation of a Novel C8-Pyrrolobenzodiazepine (PBD) Adenosine Conjugate. A Study on the Role of the PBD Ring in the Biological Activity of PBD-Conjugates. *Molecules* **2020**, *25* (5), 1243.

35. Brosseau, C.; Colston, K.; Dalgleish, A. G.; Galustian, C. The Immunomodulatory Drug Lenalidomide Restores a Vitamin D Sensitive Phenotype to the Vitamin D Resistant Breast Cancer Cell Line MDA-MB-231 through Inhibition of BCL-2: Potential for Breast Cancer Therapeutics. *Apoptosis* **2012**, *17* (2), 164–173.

36. Yin, L.; Wen, X.; Lai, Q.; Li, J.; Wang, X. Lenalidomide Improvement of Cisplatin Antitumor Efficacy on Triple-Negative Breast Cancer Cells Inï¿½vitro. *Oncol Lett* **2018**.

37. Gribben, J. G.; Fowler, N.; Morschhauser, F. Mechanisms of Action of Lenalidomide in B-Cell Non-Hodgkin Lymphoma. *Journal of Clinical Oncology* **2015**, *33* (25), 2803–2811.

38. Thomas, B. ab I.; Lewis, H. L.; Jones, D. H.; Ward, S. E. Central Nervous System Targeted Protein Degraders. *Biomolecules* **2023**, *13* (8), 1164.

View Article Online
DOI: 10.1039/D5MD00316D

View Article Online
DOI: 10.1039/D5MD00316D

Data Availability

The data supporting this article have been included as part of the Supplementary Information.